University of Nottingham
UK | CHINA | MALAYSIA

The utilization of Delft3D model to relate the coastal hydrodynamics and water quality with the illustration of Yong River Estuary in the southeast of China

Submitted October 2022, in partial fulfilment of the conditions

for the award of the degree **MRes Environmental Science and Engineering**

Yue ZHU

20416023

Supervised by Dr. Meili FENG and Dr. Fangfang ZHU

School of Geographical Sciences

University of Nottingham

I hereby declare that this dissertation is all my own work, except as indicated in the text:

Signature_____

Date_____/_____/_____

I hereby declare that I have all necessary rights and consents to publicly distribute this dissertation via the University of Nottingham's e-dissertation archive.

Public access to this dissertation is restricted until: _____/_____/_____

ABSTRACT

Coastal rivers and estuarine systems currently face growing pressure brought on by population increase and speedy economic development, which threatens the deterioration of the water quality and water ecological environment. This study takes the example of the Yong River Estuary, which is located on the eastern coast of China and south of Hangzhou Bay, to investigate the relationship between hydrodynamics and water quality response in the coastal water. Based on the hydrodynamics and water quality characteristics of a 26-kilometre-long river network, a hybrid model is established using the open-source Delft3D model. We used the bathymetry data at a 1:10,000 scale from China Navy Hydrographic maps published by China Navigation Publications Press, water level changes data from Ningbo gauging stations, and water quality data (DO, COD, BOD_5, NH_4^+, PO_4^{3-}) during 2020 and 2021.

The proposed model has two major components including hydrodynamics modelling and water quality simulation. It reconstructs the three-dimensional temporal-spatial variations of key water quality indices in the river reach and coastal waters. Six different sampling points were chosen from the river and the nearby sea area to monitor the water quality during the period from January 2020 to December 2021. The performance of the dynamic water quality model was evaluated using the coefficient of determination (R2), the Root-Mean-Square Error (RMSE), and the Nash-Sutcliffe Efficiency (NSE) values for both the calibration and the validation periods. The hydrodynamic model provides reasonable validation of water levels and tides in the Yong River and the sea area near the estuary and provides stable flow field conditions for the water quality model. The results of the water quality model simulations are generally consistent with the measured values, providing a basis for further research into the distribution of water quality parameter concentrations in the estuary.

The results show that the hydrodynamic periodicity of coastal rivers and ocean tides has a significant effect on the distribution of water quality parameter concentrations. The flow direction and velocity of the Yong River Estuary are influenced by irregular semi-diurnal tides, and the hydrodynamic circulation in the estuary varies with the tidal conditions. The hydrodynamic circulation in the estuary can influence the transport of pollutants and the concentration distribution of water quality parameters in the estuary area changes its position in the estuary with the tide. Seasonal differences will have an impact on the tidal conditions and freshwater inflow as well, which will subsequently have an impact on the hydrodynamic circulation and the values and distribution of water quality parameter concentrations. This study provides a scientific basis for research on coastal rivers and estuarine systems. It gives support to the management of the water environment and the environmentally friendly development of the coastal waters. Although the approach is used for the Yong River Estuary in eastern China, the methodology is also applicable to other coastal areas that are affected by coastal river inflow and tidal action.

KEYWORDS: Coastal waters, Delft3D model, Hydrodynamic, Water level, Water Quality, Yong River Estuary

ACKNOWLEDGEMENTS

This thesis watches the whole progress of my Master of Research studies at the University of Nottingham, China. It has been a wonderful ride, I acquire new knowledge and got to know very interesting people. I have to say that the help and support of my professors, family, and friends have shaped me better and better. I would like to take this opportunity to express my appreciation and gratitude.

First of all, I would like to thank both my supervisors, Dr. Meili Feng and Dr. Fangfang Zhu, for all the support and patience they gave throughout the process. Special thanks to Meili for your valuable input and guidance during every meeting, and thank you very much for helping me find a suitable research topic and for applying for a stable study place at PMB with equipment. A huge thank you to Fangfang for your beneficial inspiration and encouragement, and a great thanks for approving me in this special period and allowing me to continue my study.

I would also like to acknowledge Dr. Faith Chan. Thanks to him all the leaders and endeavors to make sure the successful running of the MRes program. I also want to express my gratitude to the teachers working in the Graduate School office for their understanding and willingness to assist and find solutions.

In particular thanks to my friend Tian, Guoman, Jing, Dave, and Shuyi for their presence and support, for the talks and many discussions. Thank you to Shuyang for your ongoing help and the pleasure you offer, and always fill our lives with laughter. Thanks to everyone at PMB412 and PMB423 for their kindness.

To my family and person who always has been there for me, your unconditional support drives my motivation and encouraged me to finish my studies. Finally, to my parents lovely Ms. Liu and Mr. Zhu, my endless gratitude is given to them for their constant support, accompany, and warmth. Despite the distance we are always together, I truly appreciate all the wonderful moments we have shared together, and this is for you, thank you and love you.

Yue Zhu
October 2022

Contents

List of figures

List of tables

1. Introduction

With the exploitation and depletion of land resources, more and more people are paying attention to resource-rich ocean regions. More and more companies are congregating in coastal areas, particularly in coastal cities with significant ports, as the harbours can lower transportation costs and improve revenues along coastal areas. Nearly 60% of people live within 60 kilometers of the coast on the landside of the world's nearly 50×10^5 km of coastline, and two thirds of the cities with populations greater than 2.5 million are situated close to tidal estuaries (Lakshmi & Rajagopalan, 2000; Luo, 2016; Martínez et al., 2007). The world's coastal populations make up a significant portion of the roughly 1.5 trillion-dollar global economy each year. By 2030, this amount might reach approximately 3 trillion (Kepesidi et al., 2022). However, the environment in coastal areas is becoming more polluted because of population growth, traditional industries, new marine industries, as well as an increase in the number of ships and transportation in coastal areas. The ecosystem of estuaries and coastal regions all around the world has been worse since the twenty-first century. How to effectively protect and recover the estuaries and coastal zones has been a problem which needs to be solved by all coastal counties in the world. The links between rivers, their watersheds, and the coastal ocean are the focus of an increasing number of international programs run by the International Geosphere-Biosphere Programme (IGBP), most notably LOICZ (Land-Ocean Interactions at the Coastal Zone) (van de Plassche, et al., 1995; Pernetta & Millian, 1995). Besides, Future Earth has listed the development of ocean and coastal zones as one of 13 important research areas (Liverman et al., 2013). United Nations Oceans Conference issued a declaration 'Our Oceans, Our Future, Our Responsibility' to call for urgent action to protect the marine and coastal ecosystem.

Coastal areas are the zones which have the strongest interaction between land and sea, where geophysical, chemical, biological, and sedimentary geomorphological processes and human activities are coupled with each other, which makes the coastal estuaries sensitive and complex (Chen J. & Chen S., 2002). The coastal ecosystem includes coastal plain hills, coastal rivers, estuaries, delta, coastal ponds, lagoons, harbours, docks, and other parts. Among them, environmental problems caused by the development of the coastal economy and urbanization phenomenon are more obvious in the areas of rivers, estuaries, and coastal waters. LOICZ relocated five 'research hot points' for special coastal zones including estuaries and coastal zone urbanization in 2009 (Luo, 2016). Milliman, et al. (2013) calculated that historically rivers discharge is 36,000 km^3 of water to the global coastal ocean (the mean global runoff is 350–360 mm/yr.) and more than 20 billion tons of sediments, both dissolved and solid, were added to the ocean In China, more than 80% of marine environment pollutants are brought in by rivers from the land. (Liu et al., 2017).

The water environment in coastal areas has been threatened and deteriorated by pollutants from rivers entering the sea, which seriously affect the coastal ecological

environment, business activities and marine fishery. Therefore, to realize the real-time prediction of pollutant concentrations and control deteriorating coastal water quality conditions, we need to improve the understanding of the relationship between hydrodynamic and water quality in the estuarine area and to make it possible to build a risk reaction plan and management strategy specifically suited to the condition of declining coastal water quality. The presented research is focused on assessing the impact of hydrodynamic characteristics, such as the hydrodynamic circulation of the coastal river, on water quality in the estuarine areas. Particular interests are parameters such as Dissolved oxygen (DO), Chemical oxygen demand (COD), Biochemical oxygen demand (BOD_5), Ammonium (NH_4^+), and Orthophosphate (PO_4^{3-}) that always exceed the standard and have a crucial influence on the water qualities in the estuaries and coastal zones (Ministry of Ecology and Environment, PRC., 2021).

Yong River and its estuaries are located on the southeast coast, Ningbo, Zhejiang province, close to Hangzhou Bay in the north, and Xiangshan port in the south, which is the key connection between the inner reivers and outside marine zones. Yong River Estuary, which is a very important developing area in the marine economy of Ningbo, is densely routed and has many terminals and harbours. Yong River is close to Zhoushan fishery harbour, rich in aquatic resources, has good breeding conditions and diverse ecological types. It is not only an excellent place and habitat for breeding and fattening fish, shrimp, shellfish, algae, and other marine organisms, but also a significant marine aquaculture base in Zhejiang province. This region's industry is developing diversely and includes recreational tourism, cultural production, aquaculture, equipment manufacturing, and other activities.

However, with the rapid development of the marine economy, population and industries, the increase of ships, and sewage discharge during the activities of industries manufacturing, aquaculture and agriculture, the ecological environment in this area is getting worse and worse (Wu, 2020). Dissolved inorganic nitrogen and active phosphate are the main matters that cause the pollution in the Yong River Estuary and its coastal areas in Zhejiang province, the largest source of pollutant comes from total Nitrogen and Phosphorus from land-sources, the water environment is in the state of heavy eutrophication. From 2021 Zhejiang Province Ecological Environment Status Bulletin (Department of Ecology and Environment of Zhejiang Province, 2021)，it can be clearly seen that the water quality is very poor in the areas of Yangtze River Estuary, Hangzhou Bay, Yong River Estuary and the coastal waters along Zhejiang，and the area of inferior Class IV water quality is 16,310 km^2 (Figure 1). The main exceeding indicators are inorganic nitrogen and active phosphate. The overall state of Yong River Estuary and coastal water is heavy eutrophication, the water environmental quality is mainly threatened by pollutant that rivers import under the background of urbanization and rapid development of industries and agriculture.

Based on the significantly meaningful pollution prevention in the coastal water environment of Ningbo, it is necessary to use the numerical simulation to analyse the

hydrodynamic characteristics of coastal water and to predict the effect on the distribution and seasonal differences of water quality parameter concentrations in Yong River Estuary. This research aims to set a hydrodynamic and water quality model by using Delft3D in Yong River and its estuary area to analyses the relationship between hydrodynamics and water qualities, and to understand relevant water quality influencing factors in the complex estuarine water environment.

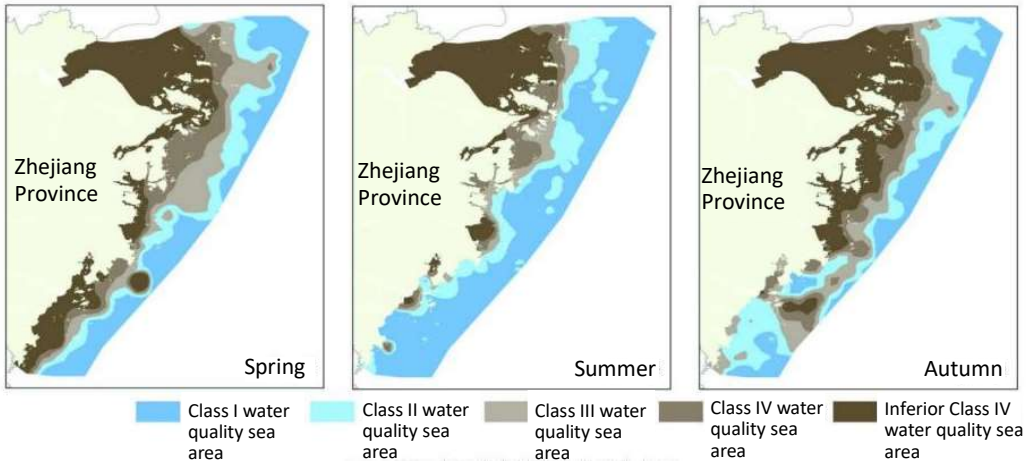

Figure 1. Distribution of seawater categories in Zhejiang Province (China) coastal waters in 2021 (Department of Ecology and Environment of Zhejiang Province, 2021).

2. Literature Review

2.1 Estuaries and coastal rivers

An estuary is a semi-closed coastal water feature with a free connection to the ocean where freshwater from land drainage is measurable diluted with seawater (Pritchard, 1967). Coastal rivers are the main source of freshwater, which is mixed with saltwater as tides rise and fall. Coastal water is typically defined as the area of the ocean that is affected by its closeness to land, which has a discernible impact on the water. For the sake of simplicity, estuaries are where rivers meet the ocean, while coastal waters are where land meets the ocean (Ji, 2017).

As one of the important economic activity zones, the coastal estuary system is the main transition zone or ecotone between the riverine and marine habitats. They are ephemeral systems with dynamic geomorphology that are impacted by both land and sea changes (Alipoor et al., 2011). For estuaries, the geomorphology dictates characteristics, such as the difference depth and length of the estuary and conditions at the upstream boundary. These factors can all influence tides (example for the type of tidal wave, the tidal heights, and the phase between current velocities), freshwater inflows, and stratification. For instance, sills and shallow channels promote vertical mixing; deep channels are more prone to stratify and have prolonged upstream salinity intrusion. The circulation and flushing of bottom waters may be impeded by shallow sills at an estuary's mouth. Narrow constrictions boost vertical mixing and velocities, but narrow inlets limit tidal movement (Alipoor et al., 2011). The difference of estuary geomorphology has a significant impact on the movement of pollutants according to control estuarine circulation and ultimately impacts water quality characteristics. Hence, it is meaningful to study pollutant diffusion according to the characteristics of estuaries.

To further understand the influence of geomorphological characteristics on estuarine hydrodynamics and water quality, a systematic geomorphological classification of estuaries should first be mentioned. Estuaries can be categorized into four groups by using the basic morphological definitions according to the Pritchard's classification in 1960, they are Drowned River valleys (coastal plain estuaries), Fjords, Bar-built estuaries, and Tectonic estuaries, respectively (Pritchard, 1960).

Estuaries on coastal plains are typically wide and shallow (rarely deeper than 30 m), with gently sloping bottoms, depths rising steadily toward the outlet, and significant deposits of sediment. Such estuaries are normally drowned river valleys (Perillo, 1995) which have a funnel shape with a more open V-shape, and the cross-section grows exponentially towards the mouth. As a result, pollutants deposition can happen readily in this type of environment. The Yangtze River is one of the typical estuaries with varying degrees of heavy metal sedimentations, such as Cu, Zn, Pb, Ni, Mn, and Fe. Zhang et al. (2001) took samples of the water quality in the area and discovered that sediments altered with time and space, and that a portion of the concentration of heavy

metals in some tested places relies on the practical size. Thames Estuary is a different well-known estuary that the high concentration of P in coastal estuarine sediments can easily cause eutrophication in coastal areas. Andrew et al. (2018) measured the concentration and morphology of P in this area and discovered that the concentration of sediments greatly depends on the regional location. Part of sediments concentration is high in some areas because of kinetics and water chemistry, which is easy to exacerbate the degree of eutrophication in the estuary.

Fjords are generally long and narrow with steep sides and relatively deep waters (Martin et al., 1999). Width-to-depth ratios are commonly less than 10:1. Fjords typically have shallow sills at the estuarine mouth and are strongly stratified, resulting in hypoxia (or even anoxia) in deep waters. These factors frequently restrict circulation and mixing in deep water, severely impede flushing, and only allow the surface waters to be affected by tidal forcing. Fjords are typically created by glacial and can be found, among other places, in Alaska, British Columbia, and Norway. Fjords like Puget Sound in Washington State are one type of estuary.

Bar-built estuaries which is called coastal lagoon as well are bodies enclosed by the deposition of a sand bar off the coast. Bar-built estuaries are generally shallow (a few meters deep or less), and the lagoon has relatively short and wider closed barrier with little tidal range and river flow where wave action suspends sediments for transport along the coast. At the same time, bar-built estuaries are typically unstable, vulnerable to cyclical and slow changes in concentration, vertically well mixed, and heavily influenced by wind. Salinities are typically higher than in other estuaries because to evaporation, limited mixing with the open ocean, and low rates of freshwater inflow.

Tectonic estuaries are produced by tectonic activity, faulting, landslides, or volcanic eruptions (Chin, 2012). Although these estuaries share some geographical traits and cause of formation, the pollution situation is highly varied due to regional climates and other factors. An example is San Francisco Bay, which was formed as a result of the San Andreas Fault's movement. In the area of San Francisco Estuary, the concentrations of Cr, Hg and Ni are higher than the water quality standards (Mills, 1985). Thompson et al. (2000) detected that the concentration of heavy metals is usually higher than standard values with no decreasing trend in the San Francisco Estuary Regional Monitoring Program for Trace Substances, the main reason is the pollutants flows from the cities to the sections of bays.

To acquaintance the classification schemes are useful for comparing different estuaries and for predicting the characteristics of a particular estuary, assisting to identify the driving forces for estuarine circulation and aid in the selection of modelling approaches. River flow and tidal action are the main forces behind the transport and circulation processes in estuaries. Ocean tides often dominate the mixing of the water body in estuaries (Gross et al.,1972). The interaction of the gravitational forces of the moon, sun, and, to a lesser extent, other planets is what primarily causes the ocean tides. A

considerable part in the transfer of pollutants can be played by residual circulation patterns with minor magnitude but great persistence that are produced by the interplay of the tides with other driving forces and terrain.

At the same time, freshwater flowing into an estuary normally also has a significant impact on mixing. Some estuaries contain enough freshwater to maintain a density differential over long distances before mixing fully with the seawater. Due to these density disparities, flow patterns are created that tend to keep the density differences. High gradient regions, such as the pycnocline and salinity fronts, prevent localized mixing and can lead to "pools" of fresher water that are confined to a particular stretch of the coast (Martin et al., 1999). Examples include the South Atlantic Bight's cleaner water band, which is constrained to an area of land within 15 km, and the Chesapeake Bay Plume (Georgia and the Carolinas). These waterways may contain pollutants for fairly lengthy periods of time after they are introduced. (Martin et al., 1990). An estuary's characteristics might shift from being well-mixed to being partially mixed or stratified as a result of increased freshwater influx. Reduced input can have the opposite impact by causing an increase in seawater incursion upstream. Such changes near an outfall can change the degree of effluent mixing. Freshwater inflow fluctuates mostly on a seasonal basis, but large amounts of freshwater can be introduced to estuarine systems by severe storms, especially during late summer and fall (Martin et al., 1999). Circulation patterns frequently respond to changes in freshwater flow but vary according to the type of estuary.

Apart from the impact of geomorphology and nature dynamics, the surrounding natural environment of estuaries are also very sensitive to human influence. Due to the majority of urbanization occurring in the coastal area, human pressure and influence on estuaries are particularly considerable (Meire et al, 2005). Throughout the world, most densely populated metropolises are built in estuaries with fertile land and natural geographical advantage (Martínez et al., 2007). Frequent human activities at estuarine area have exacerbated the pollution of coastal water (including coastal rivers, estuaries, and sea) (Neal et al., 1998; Webb et al., 1997; Wu et al., 2004). Many estuaries contain important harbours, ports, and navigatrices channels, where various ships dock to load and unload cargo, pick up and drop off passengers. Due to the large number of ships and the high frequency of shipping, the water quality around the harbour is also face a great risk of the oil and heavy metal pollutant (Huang et al., 2013; Qin et al., 2016; Xing et al., 2018).

Many estuaries flush municipal and industrial wastewater out to sea. Studies show that more than half of the dissolved elements in the ocean, such as nitrogen, phosphorus and silicon, are carried and imported from rivers entering the sea (Benitez-Nelson, 2000; Zhang et al., 1999), and this phenomenon is more prominent in watersheds with frequent industrial and agricultural activities. Shepherd et al. (2007) and Bricker et al. (2014) used simulation to get the value of the nitrogen input and the amount of dissolved and granular trace elements from rivers to estuary, such as aromatic, copper, lead and zinc in the Potomac River Estuary and Humber estuary. They found that the

river source contributed little to the nitrogen input at Potomac River Estuary and Humber estuary, and most of the number of pollutants in the coastal estuary was due to mining, industrial activities, and urbanization.

Estuaries also are biologically productive bodies of water. They are important zone for fisheries and aquaculture industry. The fishing and aquaculture industries have a great impact on output, but they are also a major contributor to the decline of aquatic ecosystems in areas where people live. Due to the bait wastes and high-density farming technique, the fishery based on aquaculture has a negative impact on the ecosystem. Njiru et al. (2012) used a model to analyse the data gathered on the water quality of the Fisheries in the Victoria and discovered that microorganisms in the water accelerated some chemical reactions like denitrification-nitrification due to the rising water temperature, which had some effects on the cycle and availability of nutrients. At the same time, the growth in seaweed caused a significant loss of oxygen in the water, leading to severe deep-water hypoxia.

2.2 Hydrodynamic and water quality models

Hydrodynamic and water quality models are used as an additional tool to assist the researchers to explore the relationship between the hydrodynamic characteristic and water quality in estuaries. Historically, scaled physical models housed in large hydraulics laboratories and field observation (including radar buoy ocean remote sensing station and seabed foundation, etc.) are the main means of studying nearshore hydrodynamic and water quality characteristics. However, physical models and the approach of field observation have a number of major drawbacks for water quality simulation. For the field observation technology, it has the disadvantages of high observation cost and limited coverage. For the physical models, there are a number of important drawbacks for water quality modelling, such as inflexibility, distorted scaling of parameters, cost, and non-adaptability. For example, in that changes in geometry, topography, and hydrodynamics are difficult to include and in that such models require large and well-equipped laboratories (Wrobel & Brebbia, 2012). Water engineers and scientists are increasingly using numerical hydraulic and water quality models for investigations of water pollution due to the limitations of field observation and physical hydraulic models as well as the quick advancements in computer technology. With the continuous development of computational fluid dynamics, hydrodynamic and water quality models also gradually shift from single-dimensional models to three-dimensional model studies, and from a single steady-state, point-source model to a comprehensive dynamic coupled model.

Hydrodynamic model

The study of hydrodynamic models dated back to 1871, Saint-Venant equations were proposed by the French scientist Saint-Venant. The core theory of the model is to use the conservation of mass and momentum equations to describe the motion characteristics of water flow in various shallow water bodies with free surfaces.

Hydrodynamic studies in estuarine coastal regions have been developed since the 1950s (Davies et al., 1997). In 1956, Hansen used the Navier-Stokes equation's (the N-S equation) solution to create a one-dimensional vertical model to examine gravity circulation in the strait and estuarine areas (Richards, 1980). In order to verify the effects of saltwater intrusion on the upstream channel flow and channel depth, Festa and Hansen (1976) added a longitudinal dimension along the estuary direction to the one-dimensional model. They then used this two-dimensional model to confirm a phenomenon of landward movement of the channel depth deepening due to saltwater intrusion. In 2003, Xu and Liao (2003) used the finite element method to simulate the hydrological variability of the Huangpu River's mainline and created a two-dimensional hydrodynamic model as a result. A model for pre-tidal variability in the Gironde estuary, France, was created by Huybrechts et al. (2012) using an improved finite element numerical calculation method for two-dimensional hydrodynamic prediction. A novel box model method was created by Officer et al. (1980) to simulate water, salinity, and continuum transport. The seaward flow of estuarine currents in a two-layer system can be simulated using the Officer's box model. It could stand in for the gravitational circulation phenomenon, which foresees salinity bands between layers, bottom-layer motion toward land, and surface-layer motion toward the sea. However, in practice, estuaries are not suitable for depth averaging because of the complex underwater topography and high elevation variability, which requires 3D models. Based on the Alternating Direction Implicit approach (ADI), Kim et al. (2010) developed a numerical model of tides and salinity in a three-dimensional bay for relevant studies. Lai (2002) successfully applied the calculation of the coupled hydrodynamic-water quality model connecting a one-dimensional river network and a three-dimensional estuary for the first time in the Pearl River estuary in 2002. In order to simulate various flow fields in the Pearl River Estuary, Long and Lee (2007) employed the finite element approach in 2007. A combined one-dimensional salinity and three-dimensional layered oblique pressure model was developed in the Pearl River estuary by Hu and Lee (2008), which was successful in describing the typical hydrodynamic processes in the Pearl River Delta.

Leendertse and Liu (1975) used fixed stratification in the vertical direction to convert a three-dimensional problem into a two-dimensional problem for treatment in a three-dimensional numerical model of a coastal estuary. To verify the effects of saltwater intrusion on the upstream channel flow and channel depth, Festa and Hansen (1976) added a longitudinal dimension along the estuary direction to the one-dimensional model. Using this two-dimensional model, they were able to confirm a phenomenon in which the channel depth moved landward as a result of saltwater intrusion. Warner et al. (2005) showed how to employ 3D models to capture tides and sub-tides on temporal scales by studying stratification during spring and flat tides at the Hudson River estuary.

Ralston et al. (2010) employed an unstructured grid to simulate the Merrimack estuary and showed that the variability of the simulated salt flux is significantly influenced by the resolution of the underwater topography used in the simulation. In Willapa Bay,

Washington, Olabarrieta et al. (2011) created a wave-flow interaction model and discovered that waves significantly affect how water bodies interact with the coast and estuary during storm surges. Through numerical models, Kuang et al. (2009) deduced that extensive reclamation had an impact on the peak flow reduction in Victoria Harbour. Wei et al. (2010) examined how Sanggou Bay's hydrodynamic features affected its capacity for aquaculture and discovered that aquaculture has a significant impact on the hydrodynamics' vertical structure.

Water quality model

Since 1960, water quality models have been steadily developing because of increased biochemical and physical understanding, as well as the advancement of computer technology. The depth of the description of natural processes, the source and sink words, and the efficient use of the powerful processing capacity of the computer were all steadily added to the water quality model. Coupled hydrodynamic-water quality models have been widely employed in estuarine and coastal engineering sectors, becoming a significant tool for predicting the status of the water environment due to the rapid development of numerical solution techniques for partial differential equations (Xu & Liao, 2003).

Water quality modelling originated in 1925 with the Streeter-Phelps oxygen balance model, known as the S-P model, which was developed by Streeter and Phelps to study the sources of pollution in Ohio rivers and river water quality to control river pollution (Phelps & Streeter, 1958.). Streeter and Phelps found that when a river is polluted, the amount of dissolved oxygen obtained from surface reoxygenation of the water body and the decomposition of organic materials in the water body uses the same amount of dissolved oxygen. They discovered that until the discharge of organic matter is reduced, the amount of dissolved oxygen obtained from surface reoxygenation in a polluted river does not equal the amount of oxygen consumed by the degradation of organic matter in the water body. This finding shows that the reoxygenation process at the water surface is a significant source of dissolved oxygen in the water body. Under the current water pollution conditions, it also accurately computed the dissolved oxygen concentration downstream of the river. Many people have since made improvements to the S-P model, including O'Conner (1967), who did so by taking into consideration the dispersion coefficient, the carbon biochemical oxygen demand (CBOD), the nitrification biological oxygen demand (NBOD), and other factors. The S-P model was enhanced much more. Howland and Thomas (1949) added a flocculation factor to the steady-state S-P model, suggesting that substrate oxygen consumption should be deducted from CBOD oxygen consumption because it is an oxygen-consuming process just as turbulence. Dobbins (1964) expanded upon Howland and Thomas's model by include plant respiration, runoff-DO relationships, photosynthesis, runoff-DO correlations, and the process of reoxygenation of the substrate.

The cycling systems of nitrogen and phosphorus in the water column, as well as plant and animal systems, had been incorporated by the 1970s and 1990s, and biological

growth rates had been treated as a function of environmental variables in the water column. Water quality models had also evolved from being one-dimensional to two-dimensional and from linear to non-linear (Blumberg & Mellor, 1987). The finite difference approach and the finite element method were also included to the solution of one- and two-dimensional water quality models with the addition of non-linear models. Since the 1990s, when significant land-based sources of pollution such heavy metals, nutrients like nitrogen and phosphorus, diverse organic and inorganic pollutants, and hazardous compounds were included to the framework of water quality modelling, the methodology has been gradually improved (Needham et al., 1993).

When compared to physical models and field observations, numerical models are often far more flexible, transportable, and adaptable, and they replicate flow and pollutant transport processes at the prototype scale. However, there are drawbacks to numerical hydraulic models as well. Intricate differential equations regulating the conservation of mass and momentum as well as the advection and diffusion of contaminants must be solved as part of numerical simulations. Hence, numerical models always call for a high level of technical skill. The follow gives the governing equations and solution procedures of general hydrodynamic and water quality models.

The calculation method of hydrodynamic and water quality models

The governing hydrodynamic equations of motion for flow on a rotating earth must first be solved in order for numerical models to anticipate flow and pollution transport processes in coastal and inland hydraulic basins. The velocity and water elevation fields for three-dimensional numerical models can then be derived from the Reynolds and continuity equations under the assumption of isothermal conditions and a hydrostatic pressure distribution (Wrobel & Brebbia, 2012).

In a number of flow and pollution transport model investigations, the hydraulic basin can be assumed to be vertically well mixed, such as non-stratified coastal waters, estuaries, rivers, and reservoirs. The three-dimensional equations of motion can be integrated over the depth to convert the hydrodynamic model to a two-dimensional depth integrated type of model. The broad definition of the advective-diffusion equation also can be added to the appropriate hydrodynamic model in order to solve for a variety of water quality parameter distributions using the time-varying water elevation and velocity fields that were obtained by solving the related two-dimensional or three-dimensional depth integrated equations numerically.

Numerical model solution procedures

Following the development of the governing differential equations for the hydrodynamic and water quality models, these equations are primarily solved by either the finite element method or the finite difference method. The finite difference solution methodology has been far more frequently employed for such model investigations than the finite element method due to computational efficiency and low artificial diffusion.

Adopting the finite difference solution strategy, this approach typically entails creating a regular grid of squares over the area of interest, reformatting the governing differential equations using Taylor's series, and solving them for each wet grid with side length Δx. Therefore, depending on the number of dimensions and water quality factors being modelled, there are four or more governing equations for each wet grid square, including the advective-diffusion equation for each solute and the equations of continuity momentum in the x and y (and z) directions. The size of the domain will affect the number and size of the grid squares. For each wet grid square, both a bed roughness height and a local depth below datum are given, with the local depth typically specified at the corner and the bed roughness height at the center of each grid square. For each grid square and each timestep, the finite difference equations are then resolved explicitly or implicitly.

2.3 Example of Available Models

Numerical simulation technology has advanced quickly and become widely employed in recent years as a result of the constant advancement of computer technology. This encompasses all of the successes that numerical models have had in the investigation of coastal water bodies. On the one hand, the analysis of conditions under the influence of external factors, such as hydrological conditions, water flow fields, wind farm environments, etc., as well as the transmission, movement, diffusion, degradation, dilution, and other processes of pollutants in water bodies are part of the research of China's coastal water bodies. On the other hand, it also covers the evaluation and forecasting of the water environment to offer scientific support for the advancement of the work of the government or pertinent agencies in management and governance. However, at present, the numerical models used by Chinese scholars in this regard are still in the initial stage of development, and most of them are imported from overseas research methods. Currently, the following are the model software that are most frequently used in research on hydrodynamic and water quality modelling: the FVCOM model developed by Masachusetts Dartmouth University in the United States (Finite-Volume Coastal Ocean Model), and the EFDC model (The Environmental Fluid Dynamics Code) developed by the Virginia Institute of Marine Sciences (VIMS) of the University of William and Mary Dynamics Code, the series software of MIKE developed by the Danish Institute for Water Resources and The Environment (DHI), and the Delft3D (Delft3D FM Suite) model developed by Delft University in the Netherlands. Each of the aforementioned model software's unique features must be taken into consideration by researchers as they select models for their studies. The following examples of models cover a few of the specific limitations and capabilities of hydrodynamic and water quality models.

(1) FVCOM

In order to model ocean circulation and ecological processes, Changsheng Chen of Massachusetts Dartmouth State University and his research group established the Unstructured Grid Finite Volume Community Ocean Model (FVCOM) in 2000.

Currently, the finite volume approach (FVM), the finite element technique (FEA), and the finite difference method (FDM) are some of the most popular discrete methods (Chen et al., 2011). The finite volume method (FVM), which combines the benefits of finite difference and finite model in marine research, is the discrete approach employed by the FVCOM model. The FVCOM model can be precisely adapted to coastal boundaries with complicated curvature by employing an unstructured non-overlapping triangle mesh in a horizontal direction and coordinates or mixed -Z coordinates in the vertical direction (Lai et al., 2010). In the meantime, to reduce calculation time, the numerical solution is split into two modes: a long gravity out-wave mode integrated along the water depth, and an internal mode connected to the vertical flow structure (Qi et al., 2009).

(2) EFDC

The mathematical model of EFDC was created in 1996 by John Hamrick and his team at the Virginia Institute of Marine Science at the College of William and Mary using the Fortran77 programming language. Later, the U.S. Environmental Protection Agency (U.S. EPA) provided funding for the upkeep of the EFDC model since its source code is free and open source, making it easier to use (Kim et al., 2017). The hydrodynamic module, sediment transportation module, toxic chemical module, water quality module, substrate module, and wind and wave module are the primary modules that make up the EFDC model system. The hydrodynamic module, which forms the core of the EFDC model, uses a finite difference method based on operator splitting techniques to primarily solve for pressure, water depth, and velocity in three directions. The sediment transport module calculates the sediment transport equation using the finite difference approach based on the operator splitting method, just as the hydrodynamic principle. The EFDC's water quality module uses a model that incorporates the conversion of various algae, organic and inorganic nitrogen, and dissolved oxygen in the atmosphere in addition to nutrient-rich compounds made of carbon and other elements like N, P, O, and Si (Wu & Xu, 2011). The several EFDC model modules can be connected to one another. For instance, the output variables from the hydrodynamic module can be connected to other modules that deal with water quality, dangerous compounds, etc. To simulate the hydrodynamics and water quality of water bodies such rivers, lakes, reservoirs, wetland systems, estuaries, and oceans, researchers can construct one-dimensional, two-dimensional, or three-dimensional models as needed (Wang et al., 2015).

(3) MIKE series

Danish Hydraulic Institute (DHI), established in 1964, created the MIKE family of software using the ArcView platform. There are a ton of different pieces of software in the MIKE series, including MIKE11, MIKE21, MIKE3, MIKE FLOOD, MIKE BASIN, MIKE SHE, MIKE MOUSE, MIKE URBAN, and WEST. MIKE11 is mostly used in one-dimensional simulations of estuaries, rivers, river networks, and inland waters' hydrodynamics and water quality. Inshore estuaries, bays, and marine waters are simulated using two-dimensional hydrodynamic and water quality models using

MIKE21 (Ahn et al., 2019). MIKE FLOOD is a very effective connection tool when linked calculations in one and two dimensions are needed. A wide range of water resources assessment and management services are offered by MIKE BASIN, MIKE SHE is primarily integrated planning to manage groundwater and surface water, MIKE MOUSE can be used to address urban drainage issues, and MIKE NET can address other issues related to urban water supply systems. Currently, the software MIKE21 is widely used in the treatment of water resources and marine models. As the software's fundamental module, the hydrodynamic module simulates hydrological characteristics using a finite difference format to obtain values for the De Saint-Venant system of equations, and the water quality module simulates a variety of water quality biochemical indicators, such as the process of eutrophication and the migration of heavy metals from bacteria (Warren & Bach, 1992). The relatively advanced computational fluid program MIKE 21 has a robust data pre-processing capability, and after data pre-processing, researchers can partition the mesh in many ways in accordance with the topographic features of the study area. The software may evaluate and visualize water body flow during the post-treatment process in order to find the best solution and finally complete the hydrodynamic and water quality simulation of rivers, nearshore waters, oceans, and other water bodies (Xu et al., 2012).

(4) AQUATOX

The U.S. Environmental Protection Agency (U.S. EPA) created the AQUATOX aquatic ecosystem model in 2000 using the Delphi programming language. Since 2000, AQUATOX has undergone over six iterations. The most recent version keeps broadening the range of applicable terrain, including the estuarine shore. The model can examine the effects of these pollutants on different animals and plants in water bodies, such as fish, invertebrates, seaweed, etc., and simulate the transport path of pollutants in water bodies, such as heavy metals, nutrient salts, etc. to create a general ecological risk model (Park et al., 2008). The model has five parameter databases, giving users access to a wide range of pre-set model parameters. Researchers can also alter these models' parameters in accordance with their own research concerns, considerably enhancing the model's adaptability. Researchers can properly forecast the spatio-temporal variations of different contaminants in the water body using the software's simulated model, calculate the concentration of pollutants in the water body, and finally provide a thorough assessment of the ecological danger (Akkoyunlu & Karaaslan, 2015).

(5) WASP

WASP (Water Quality Analysis Simulation Program) is a water analysis simulation program developed by the U.S. Environmental Protection Agency (U.S. EPA) in 1982. After several revisions and product iterations, it has become a mature water quality model software applied under WINDOWS. WASP consists of two parts: hydrodynamic (DYNHYD) simulation and water quality (WASP) simulation. The DYNHYD program is primarily used for one-dimensional hydrodynamic simulations, in which the hydrological properties are modelled by solving a finite difference system of equations

for the Saint Venant system, generalizing the water body to be calculated into a grid form, and solving for flow rates, flows, and other parameters from the grid points. The WASP water quality module is based on mass conservation and uses the advection-diffusion mass transport equation to simulate the spatial and temporal variability of water quality (Wool et al., 2020). WASP is incredibly versatile and can be used alone with hydrodynamic parameters, in conjunction with other hydrodynamic models, or by linking to DYNHYD. This allows the user to carry out steady-state and unsteady-state analyses of water bodies in rivers, near coasts, lakes, and oceans, depending on the study area, and ultimately to derive the transport and transformation patterns of different pollutants (algal pollution, eutrophication, organic chemicals, metals and sediments) in the water (Cashel & Knightes, 2021).

(6) CE-QUAL-W2

CE-QUAL-W2 (A Two-Dimensional, Laterally Averaged, Hydrodynamic and Water Quality Model) is a hydrodynamic and water quality analysis simulation software funded and expanded by the US Army Corps of Engineers Waterways Experiment Station in 1995(Cole & Wells, 2006, p. 2). CE-QUAL-W2 consists of two main components: hydrodynamic simulation and water quality simulation. The velocity, temperature and elevation of the water body can be simulated in the hydrodynamic section. The water quality section can be simulated with one or more additions depending on the needs of the research problem(Afshar et al., 2011). The software can add a wide range of water quality variables such as suspended solids, phytoplankton, pollutants, organic sediments, dissolved oxygen, non-degradable particulate organic matter, etc. The lateral mean flow rate and mass transfer rate are produced by the discrete finite difference method utilized in the model. Additionally, by combining the CE-QUAL-W2 vertical 2D model with other mapping applications, such Tecplot, study on long and narrow water bodies is much more efficient and less expensive (Al-Murib, 2014).

(7) Delft3D

Delft3D is a software package developed by the Dehares Hydraulic Institute, formerly Delft Hydraulics, for the numerical simulation of the ocean in two and three dimensions. There are seven parts included in the software package, Delft 3D-FLOW, Delft 3D-WAVE, Delft 3D-WAQ, Delft3D-PART, Delft 3D-ECO, Delft 3D-SED and Delft 3D-MOR(Symonds et al., 2017). The two most often used modules are the hydrodynamic module and the water quality module, which not only enable 3D simulations of water bodies based on parameters like water flow, sediment, and quality, but also 2D simulations of these same aspects. There is no need to rely on external software because the two software modules, hydrodynamic and water quality, can be used independently or coupled internally. Additionally, the software logically creates orthogonal curved grids and water depth files at the grid nodes, then uses the alternating implicit (ADI) algorithm to calculate water flow problems on the corresponding grids. Finally, post-processing tools are used to obtain the data. As a result, the software includes several extremely powerful tools, including RGFGRID, QUICKIN GPP, and QUICKPLOT

(Elias et al., 2001). The software is particularly flexible to complex border terrain thanks to the Delft3D model's availability of both spherical and coordinate systems, which also significantly lowers calculation costs. Delft3D is frequently used by researchers in many nations to simulate the hydrodynamics and water quality of lakes, rivers, estuaries, and other water bodies because the model is quick and stable, the components are open source, and they can be used in conjunction with external software like MATLAB to provide more powerful simulation capabilities for more complex simulations of eutrophication and water ecology types (Lesser et al., 2001.).

Table 1. Comparison of commonly used software.

Name	**Source**	**Hydrodynamic**	**Water Quality**	**Water Ecology**	**Basin**	**Open Source Code**	**Software Visualization**
FVCOM	Masachusetts Dartmouth University	√	√	-	√	√	√
EFDC	The Virginia Institute of Marine Sciences (VIMS)	√	√	√	√	√	√
MIKE	Danish Hydraulic Institute	√	√	-	-	-	√
AQUATOX	EPA	-	√	√	-	√	√
WASP	EPA	√	√	√	√	√	√
CE-QUAL-W2	USACE	√	√	-	-	-	-
Delft3D	WL Delft Hydraulics	√	√	√	√	√	√

Notes: √ means YES, - means NO.

3. Study Area and Data Source

3.1 Study area

The Yong River and the Yong River estuary

The Yong River basin is located in the eastern coast of Zhejiang province, south of Hangzhou Bay, between longitude 120°40'-122°00'E and latitude 29°25'-30°20'N. The total catchment area is approximately 5,262.2 km^2. The basin consists of two major tributaries, the Fenghua River and the Yuyao River, and the mainstream of the Yong River formed after the confluence of the two rivers, with an average annual runoff of 3.5 billion m^3 (Figure 2.). Yong River is one of the 8 main rivers system in Zhejiang province, the mother river of Ningbo. The mainstream of Yong is plain rivers sections that is affected by tides. The mainstream of Yong River refers to the Yao River and the Fenghua River converging at the Sanjiangkou (the confluence of three rivers, the Yao River, Fenghua river and Yong River) in Ningbo City to the outlet section of Zhenhai Dayoushan, with a total length of 26 km, an average water depth of 5m, a width of 50-150 m, and a catchment area of 361 km^2 in the mainstream section.

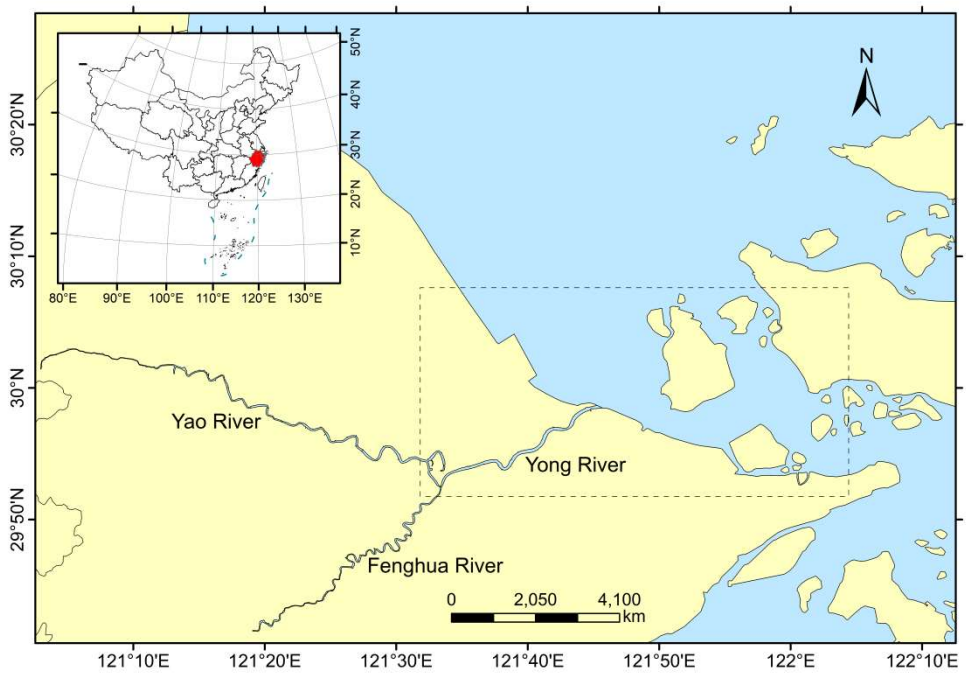

Figure 2. The Yong River basin and the black dotted rectangle indicates the modelled area.

The coast of Zhejiang province has a typical subtropical monsoon climate, which is excellent for habitation. It has four distinct seasons, a considerable winter and summer wind alternation, enough sunshine, and good temperature and humidity. At the same time, Zhejiang's coastline is abundant in different marine resources. For instance,

Zhoushan Fishery is the largest fishing area in Zhejiang's northern region. The coastal area of Zhejiang has a population density of 573 people per km^2, which is significantly higher than the provincial average value of 466 people per km^2. As a result of the favourable climate and an abundance of resources. The coastal area has become an active centre for marine economic activity, serving the needs of shipping, tourism, fisheries, industries, and other resources throughout the province and its neighbouring cities (Qi, 2021).

Zhenhai harbour area, which is primarily in charge of petrochemical, domestic trade, and coal transportation, is bordered by the Yong River Estuary on the west, while Beilun harbour area's western operation area, which specializes in ship repair and bulk and other cargo transportation, is on the east. Domestic sewage, industrial wastewater, and agricultural wastewater are all transported to the estuary's sea by the Yong River's discharge from the upstream, cities, and villages. In 2005, the total amount of pollutants carried by the Yong River and other major streams close to the Zhoushan sea area was still high, with the total amount of major pollutants entering the sea being about 6.17 million tons, including the chemical oxygen consumption that can reflect the degree of pollution of water bodies, including organic matter, nitrite, ferrous salts, sulphides, and so on, at 5.91 million tons, accounting for approximately (Jiang et al., 2011). Rivers that discharge pollutants into the sea cause an increase in the amount of nitrogen, phosphorus, and other pollutants in coastal areas, creating a unique eutrophication environment that will cause extreme red tides to coastal areas.

Furthermore, the Yong Estuary's tide is an irregular half-day shallow sea reciprocating current with a high flow rate, and the whole low tide period is longer than the total high tide time. The tide on the dockside turns back early, and the rising and falling time of main channel is larger than that of front of the dock. In addition, changes in temperature, nutrients, and organic matter in the coastal areas of the Yong estuary have resulted from the interaction of the warm Taiwan Current, the Zhejiang Coastal Current, the Yellow Sea Cold Water Group, and the West Pacific Warm Current in the coastal waters of north-central Zhejiang, further complicating the seawater affected by land-based inputs and tidal movements. A sudden change in eutrophic components is also possible. The Yong coastal estuary is becoming a typical complex aquatic environment because of several variables.

3.2 Data source

Several datasets are used for the hydrodynamics and water quality model setup, calibration, and validation. The data used in the water quality module of the Delft3D model mostly consists of monthly average water quality monitoring data. The data used in the hydrodynamic module of the model primarily consists of boundary data, underwater terrain, and real-measured water level.

3.2.1 Research domain and bathymetry

The research domain boundary is obtained by plotting in Google Earth and then transforming coordinates. The Yong River's main channel, which extends from the mouth of the Sanjiangkou to the mouth of the Youshan Inlet, as well as the surrounding sea region, are included in the research area. The grid includes the sea region west of the Sanbei Shoal to the sea north of it, north of the Cezi Island to its southernmost point, and east of the Big Cat Island to its westernmost point.

The bathymetry data we used at a 1:10,000 scale from China Navy Hydrographic maps published by China Navigation Publications Press. The data covers the Yong River from the Sanjiangkou to the mouth of the sea and then to the nearby sea area, with a total of 7,035 bathymetric points, covering an area of about 740 km^2.

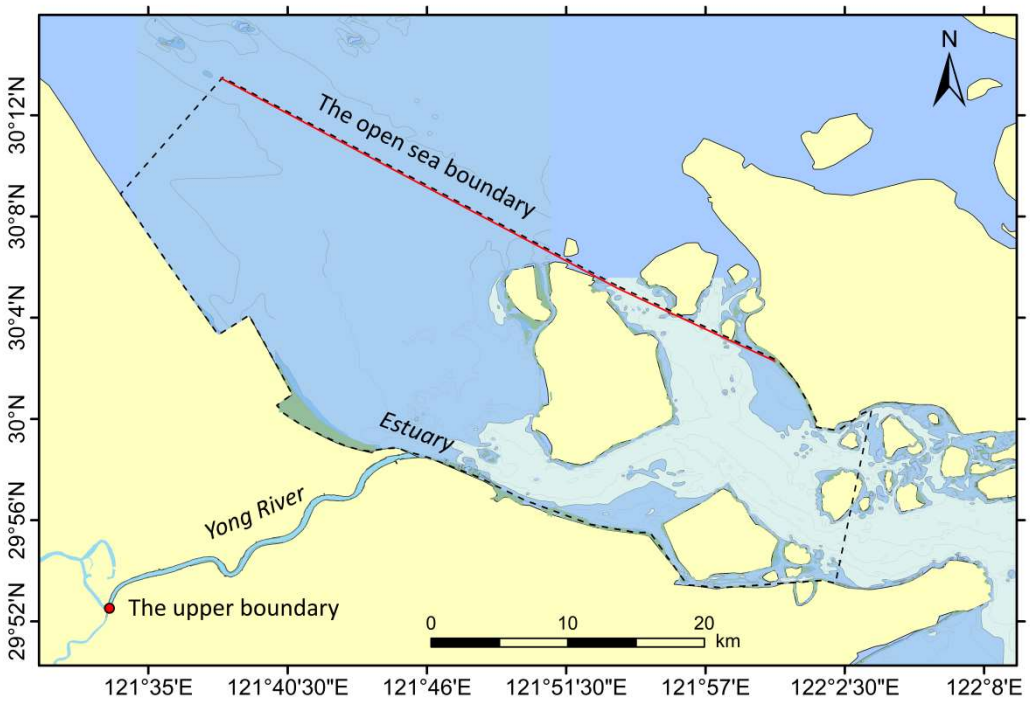

Figure 3. The mainstream of Yong River and its estuarine nearby sea area. The area that the dotted lines encompass is the area covered by model grid. The red dots and red lines are the upper river boundary and the open sea boundaries respectively.

3.2.2 Water level and tide data

Two open boundaries exist in the overall model: the upper river boundary and the seaward boundary (Figure 3). The Ningbo hydrographic station at the Sanjiangkou provides three to four daily readings of the water level for the upper river boundary. In addition, astronomic tides (combinations of a total of 35 tidal elements) produced from the global tidal model were used to specify the seaward limit as the water level boundary (OSU TPXO Tide Model Driver). The objective is to replicate the water levels at the recorded locations across a two-year tidal cycle.

In-situ Measurements

The water and tide level data used in this thesis come from three sources: the Hydrological Yearbook, the Zhejiang Province Water and Rainfall Monitoring and Warning Display Platform of the Zhejiang Hydrological Management Centre (ZJHMC, http://www.zjsw.cn/), and the Rainfall Information System of the Ningbo Water Resources Bureau (NBWRB, http://slj.ningbo.gov.cn).

In this study, the water levels at Ningbo station from 1 January 2020 to 31 December 2021, which were obtained from the Hydrological Yearbook of the People's Republic of China for the years 2020 and 2021, were utilized as input data for the upstream opening boundary of the hydrodynamic model. Two high tide points and two low tide points every day, for a total of four water level data per day, were used to collect the water level data (three water level data for individual points due to missing data). A total of five locations, including one on the Yong River's mainstream and four in the sea, were used to calibrate and validate the hydrodynamic model. The point on the Yong River channel is Wangjiayang tidal station (WL01), while the points in the offshore simulation area are Zhenhai station (WL02), Jintang tidal station (WL03), Xiasanshan tidal station (WL04) and Dinghai station (WL05) (Figure 4). The water level data for the five points are obtained from the Zhejiang Water and Rainfall Monitoring and Warning Platform of the Zhejiang Hydrological Management Centre (ZJHMC) and the Rainfall Information System of the Ningbo Water Resources Bureau (NBWRB). The daily water level data from 1 January 2020 to 8 April 2021 was collected at 8.00am at daily scale, and the specific information for each point and the respective time periods used for calibration and verification can be found in the Table 2.

Table 2. Water Level Monitoring Station Locations.

Name of the monitoring station	Data Source	Monitoring frequency	Period	Application
Ningbo	Hydrological Yearbook	3-4 /d	2020.1.1-2021.12.31	Open boundary conditions
Wangjiayang (WL01)	ZJHMC	per day	2020.1.1-2021.4.8	2020.1-2020.3 for water level calibration; 2020.4-2021.4 for water level verification
Zhenhai (WL02)	NBWRB			
Jingtang(WL03)	ZJHMC			
Xiasanshan (WL04)	ZJHMC			
Dinghai (WL05)	NBWRB			

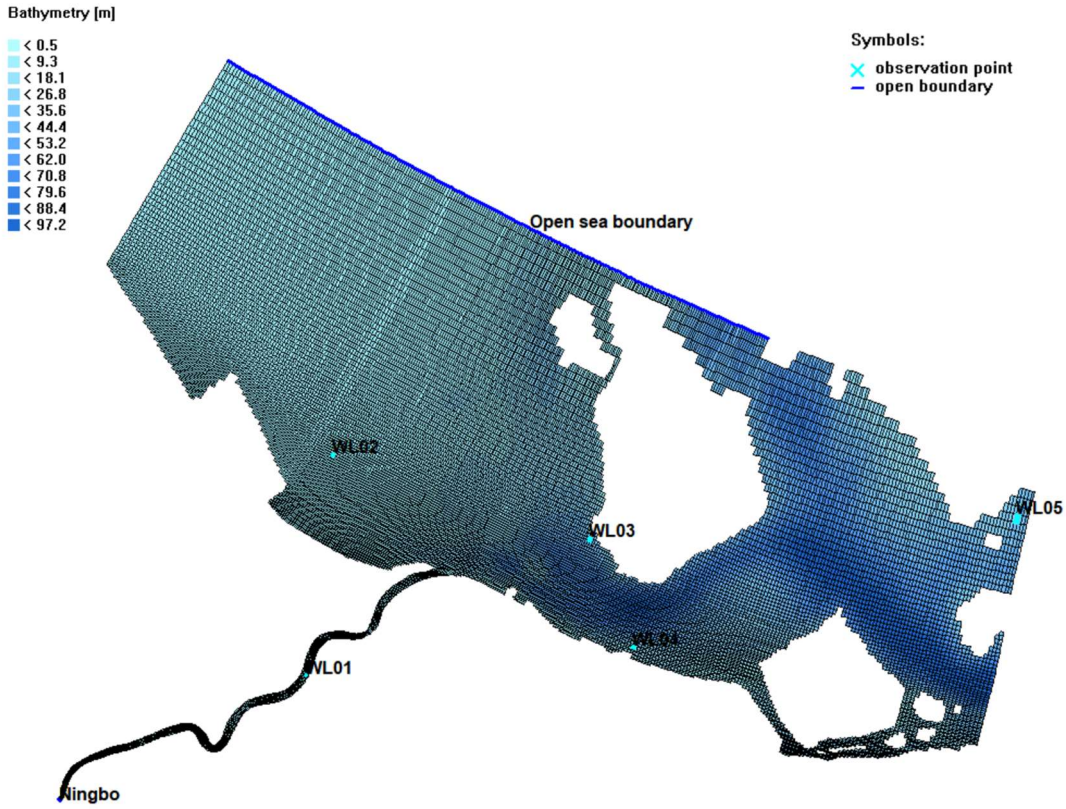

Figure 4. The five water level monitoring stations are Wangjiayang tidal station (WL01), Zhenhai station (WL02), Jintang tidal station (WL03), Xiasanshan tidal station (WL04) and Dinghai station (WL05). Two open boundaries are set for the upstream and offshore areas of the study area are the Ningbo station and the open sea boundary respectively.

OSU TPXO Global Tidal Model

The data of the tidal harmonic constants from the global tidal model (OSU TPXO Tide Model Driver) are used (Egbert & Erofeeva, 2002). The information at each station is given as tidal components, so the data can be derived at any date and time.

TPXO is a comprehensive family of ocean tidal models that use least squares and Laplace tidal equations to fit and assimilate satellite altimetry data (T/P, TopexTandem, ERS, GFO) and live tidal data (Egbert & Erofeeva, 2002). As a global, regional, and local models of barotropic tide, the global model may have similar forecast accuracy to the regional model in pelagic waters, but in shallow waters with complex topography, more data is required to improve the accuracy of the model. In the global and 24 regional models offered by TPXO, TPXO introduces high resolution topographic data (up to 1/60° spatial resolution in some sea area models) into the regional models and integrates different observations depending on local conditions, significantly improving forecast accuracy. Each next model in the TPXO series is based on the latest bathymetric data, incorporating more data than previous versions. For example, compared to TPXO8, TPXO9, launched in 2016, is a further assimilation update in

terms of both seabed topographic data and bathymetric information, and is the latest global solution with 1/30-degree resolution. A combination of the basic 1/6-degree global solution TPXO version 9.1 and 1/30 degree resolution local solutions for all coastal areas (including the Arctic and Antarctic) with the addition of 2N2 and S1 split tides (Egbert & Erofeeva, 2002).

In the TPXO tidal model, there are three main components: the bathymetry/depth grid (m), the elevations (m), and the transports (m^2/s). It is important to note that tidal elevations and transports are expressed as complex amplitudes, which means that for a single constituent of frequency w at location x, the partial tide at time t is given by the formula:

$$h(t,x) = pu(t,x) \cdot Re[h(x)exp\{i[w(t-t_0) + V_{0(t_0)} + ph(t,x)]\}] \quad (1)$$

where,

$V_{0(t_0)}$ the astronomical argument for the constituent at time t_0,

$pu(t,x)$ and $ph(t,x)$ nodal corrections.

Then amplitude = | h | and phase = atan (-Im(h)/Re(h)). Since tidal elevations are referenced to mean sea level (MSL), long-term averages of model time series are zero. The TPXO model includes complex amplitudes of MSL relative to sea surface height and transmission/currents for eight majors (M2, S2, N2, K2, K1, O1, P1, Q1), two long period (Mf, Mm) and three non-linear (M4, MS4, MN4) harmonic components (only TPXO9 also has 2N2 and S1) (Egbert & Erofeeva, 2002). In this study, eight major harmonic components (M2, S2, N2, K2, K1, O1, P1, Q1) were selected based on the tidal characteristics of the coastal waters of Zhejiang.

Table 3. The eight major harmonic components of start A and end B of the open sea boundary of model.

Location	A		B	
Parameter Con	Ampl/MajAxis Phase(o,GMT)	MinAxis Incl(o,GMT)	Ampl/MajAxis Phase(o,GMT)	MinAxis Incl(o,GMT)
M2	0.7468	114.08	0.8113	89.16
S2	0.3245	149.93	0.3628	126.34
N2	0.1124	91.31	0.1305	69.09
K2	0.0830	154.41	0.0916	126.55
K1	0.2252	116.89	0.2376	108.47
O1	0.1437	88.48	0.1566	79.14
P1	0.0613	119.38	0.0663	109.02
Q1	0.0175	73.91	0.0196	60.80

3.2.3 Water quality data

In this study, a total of eight water quality monitoring points were used in the water quality model, including three on the river and five in the sea (Figure 5.). The three water quality monitoring points on the river channel are Sanjiangkou (WQ01), Zhangjianqi (WQ02), and Youshan (WQ03), of which Sanjiangkou (WQ01) is located just at the upstream boundary of the mainstream of the Yong River, and its water quality data is used as input to the upstream opening boundary of the water quality model, and Youshan (WQ03) is located at the mouth of the Yong River. The water quality data for these three sites are monthly averages for 2020 and 2021 and include water quality parameters such as PH, DO, COD, BOD_5, T-P, and T-N, obtained by application from the Department of Ecology and Environment of Zhejiang Province (ZJEE, http://sthjt.zj.gov.cn). The water quality monitoring points in the outer sea are ZJD12012, ZJD02013, ZJD02018, ZJD02019, and ZJD12014, where ZJD12012 is located at the boundary of the outer sea, and its water quality data is used as the boundary input of the outer sea of the water quality model, and the water quality data of other points are used for the calibration and validation of the model. These five points are located in the outer sea water quality monitoring data for 2020 and 2021 in different quarters of the year three months of monthly average water quality, including water quality parameters are PH, DO, COD, inorganic nitrogen, and reactive phosphate. The data are provided by the Environmental Knowledge Service System (EKSK) of the Engineering Science and Technology Knowledge Centre of the Chinese Academy of Engineering, developed, and built by the Chinese Academy of Environmental Sciences in 2015.

Table 4. Water Quality Monitoring Station.

Name of the monitoring station	Data Source	Monitoring frequency	Period	Application
Sanjiangkou (WQ01)	ZJEE	Monthly	2020-2021	Open boundary conditions
Zhangjianqi (WQ02)				Water quality verification
Youshan (WQ03)				
ZJD02013	EKSK	Quarterly		Water quality verification
ZJD02018				
ZJD02019				
ZJD12014				
ZJD12012				Open boundary conditions

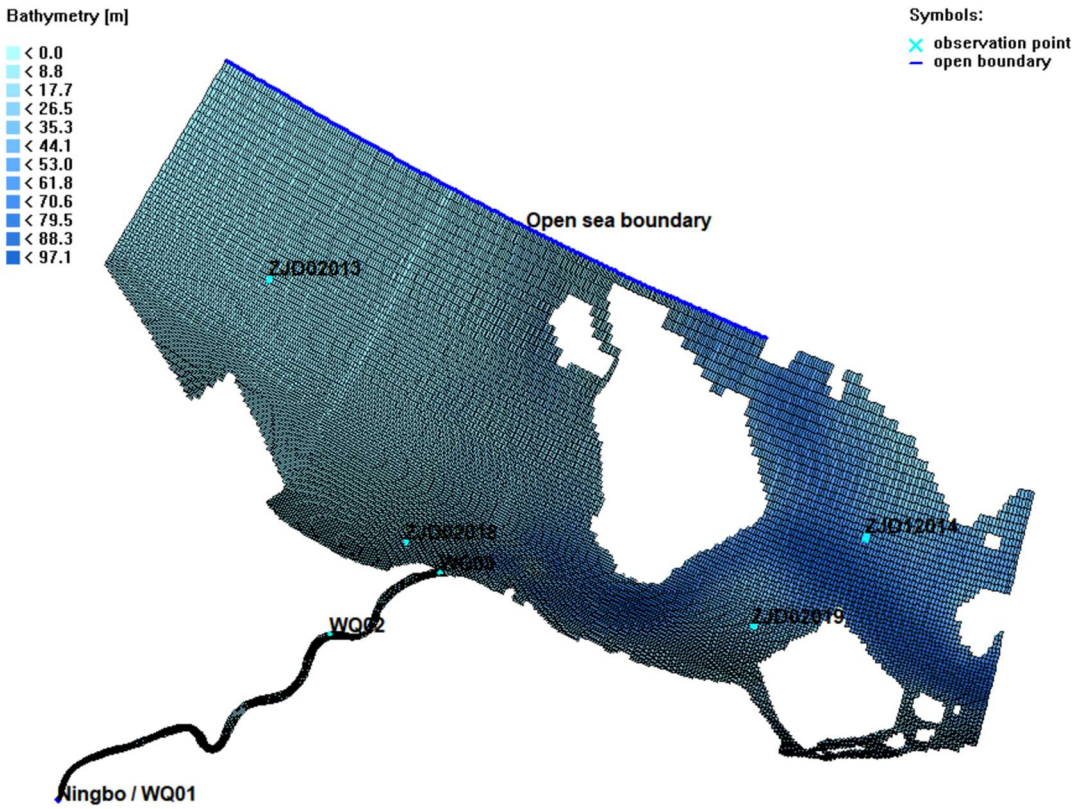

Figure 5. The location of six water quality monitoring points and two open boundaries.

4. Methodology

4.1 Delft3D Model

Delft3D modelling software is applied in this study. It is an exceptional, completely integrated set of computer tools for multi-disciplinary research and 3D computations which was developed by Deltares (Delft, Netherlands). Delft3D is mainly used in the free surface water environment in coastal, river and estuarine areas. The Delft3D suite is composed of seven modules, including the core module Hydrodynamic Module (FLOW), the Water Quality Module (WAQ), the Sediment Transport Module (SED), the Wave Module (WAVE), the Particle Tracking Module (PART), the Ecology Module (ECO), and the Bedside Morphodynamics Module (MOR) (Deltares, 2017).

The software has a flexible framework, each module can be executed separately, and the solved problems can cover specific aspects of research or engineering problems, or combined with a couple of other modules. Using the above seven main modules, Delft3D can specifically simulate the two-dimensional (horizontal or vertical surface) and three-dimensional temporal and spatial changes of water flow, water movement, water quality evolution, biological action, bed bottom landform change, and sediment transport. The two modules FLOW and WAQ are used in this thesis. In the following sections, we describe the basic principles and assumptions of each module, the controlling equations of the model, and the numerical solution methods.

4.1.1 Delft3D-FLOW (Hydrodynamic Module)

The Delft3D FLOW modelling suite is a multi-dimensional (2D or 3D) hydrodynamic (and transport) simulation program used for computing the hydrodynamics of coastal, river, and estuarine systems (Deltares, 2017). This module integrates tidal and climatic effects and calculates no-steady flow and transport phenomena using a rectilinear or a curvilinear, boundary fitted grid. Delft3D's main areas of application include tide and river flow simulations, wind-driven flows, stratified and density driven flows etc. Delft3D FLOW solves the three-dimensional, non-linear, shallow water Navier-Stokes equations to simulate hydrodynamics. The solved equations include the continuity equation, transport equations for conservative constituents, and horizontal equations of motion. In the 3D simulation, the vertical grid is defined following the σ co-ordinate approach so that the number of vertical layers remains constant throughout the computational field, which can greatly improve computational efficiency (Deltares, 2017). The basic requirements for hydrodynamic modelling include conservation of momentum, energy, and mass, but there are still many difficulties in applying strict conservation equations to numerical simulations of water bodies at large time and space scales, and most solutions are usually simplified equations that introduce various approximation conditions. The Boussinesq assumption and the hydrostatic pressure assumption are currently two widely used approximations in surface water modelling.

Fundamentals and assumptions

(1) Boussinesq assumption.

In the conservation of momentum, changes in density do not have a significant effect on the fluid properties, and they have negligible effects on the viscous force term, the pressure difference term, and the inertial force term, while only the impact on the mass force term is taken into account. Boussinesq approximates that only density changes need to be considered in the buoyancy term of the equation, the other terms are negligible, and the water flow is assumed to be incompressible.

(2) Hydrostatic pressure assumptions.

For most bodies of water with shallow water characteristics, the horizontal scale exceeds the vertical scale by a wide margin. The hydrostatic pressure assumption that the pressure gradient in the vertical direction is balanced by buoyancy and the term of vertical acceleration is ignored in the calculation, so that the hydrostatic pressure equation is a simplified version of the pressure term in the vertical momentum equation.

Control equation and calculation method

In order to reflect the 3D characteristics of the coastal harbour waters, Delft3D-FLOW uses a σ -coordinate system in the vertical direction, defined as follows:

$$\sigma = (z-\zeta)/(d+\zeta) = (z-\zeta)/H \tag{2}$$

with,

Z	vertical coordinate,
ζ	water level above the reference plane (z = 0),
d	depth of water below the reference plane (z = 0),
H=d+ ζ	total water depth.

At the bottom of the riverbed, the value of σ is -1 and at the free water surface, the value of σ is 0.

Based on Boussinesq assumptions, hydrostatic pressure assumptions, the continuity equation averaged along the depth and the 3D momentum equation are:

Continuity equation averaged along the water depth：

$$\frac{\partial \zeta}{\partial t} + \frac{\partial[(d+\zeta)U]}{\partial x} + \frac{\partial[(d+\zeta)V]}{\partial y} = Q \tag{3}$$

with,

ζ	water level[m],
d	water depth[m],
t	time[s],
U, V	the mean vertical velocities in the x and y directions[m/s],
Q	the change in water volume per unit area due to drainage, diversion, evaporation or rainfall[m3/s].

Momentum equation in three dimensions:

$$\frac{\partial u}{\partial t} + u\frac{\partial u}{\partial x} + v\frac{\partial u}{\partial y} + \frac{\omega}{d+\zeta}\frac{\partial u}{\partial \sigma} - f_v = -\frac{1}{\rho}P_u + F_u + \frac{1}{(d+\zeta)^2}\frac{\partial}{\partial \sigma}(\upsilon_V \frac{\partial u}{\partial \sigma}) \quad (4)$$

$$\frac{\partial v}{\partial t} + u\frac{\partial v}{\partial x} + v\frac{\partial v}{\partial y} + \frac{\omega}{d+\zeta}\frac{\partial v}{\partial \sigma} - f_u = -\frac{1}{\rho}P_v + F_v + \frac{1}{(d+\zeta)^2}\frac{\partial}{\partial \sigma}(\upsilon_V \frac{\partial v}{\partial \sigma}) \quad (5)$$

$$\frac{\partial \omega}{\partial \sigma} = -\frac{\partial \zeta}{\partial t} - \frac{\partial[(d+\zeta)u]}{\partial x} - \frac{\partial[(d+\zeta)v]}{\partial y} + H(q_{in} - q_{out}) + P - E \quad (6)$$

with,

u, v, ω	flow velocities in the x, y, z directions[m/s]
f	the Coasean force parameter[1/s]
P_u and P_v	the static pressure gradient[kg/m^{2}s^2]
F_u and F_v	the radiation stress[m/s^2]
υ_V	the vertical eddy viscosity coefficient[m^2/s]
H	water depth[m]
q_{in}, q_{out}	the inflow and outflow per unit volume[1/s]
P, E	the rainfall and the evaporation per unit area, respectively[m/s]

The model calculation is based on the staggered grid ADI approach, which divides a time step into two phases, each consisting of half a time step. The Delft3D-FLOW module discretizes data using the finite difference method. The model equations are all solved with spatial second-order precision for all terms. The ADI technique has the advantage of having a reduced bandwidth set of equations because the implicitly integrated water level and velocity are related along the grid lines.

4.1.2 Delft3D-WAQ (Water Quality Module)

A multi-dimensional framework for a water quality model is called Delft3D-WAQ. On a predefined computing grid, it resolves the equation of advection diffusion-reaction for a variety of model substances. When it comes to the materials that can be modelled and the processes that can be considered, D-Water Quality is incredibly flexible. Since D-Water Quality lacks a hydrodynamic model, Delft3D-FLOW is used to obtain information on flow fields (Deltares, 2017).

The Delft3D-WAQ module represents the physical-biochemical transformation relationships between various substances in a water body by solving the convection-diffusion-reaction equations (Deltares, 2020). In contrast to hydrodynamic models, water quality models require multiple disciplines to be related, with complex and numerous empirical water quality equations and various physical parameters. Many of these parameters cannot be obtained directly or indirectly, so water quality modelling needs to highlight the main substances and chemical processes of interest, while also

requiring appropriate rational simplifications and approximations. The ultimate core problem of all water quality models is to solve the convection-diffusion-reaction equation (Deltares, 2020). WAQ solves the convection-diffusion-reaction equation on the basis of a well-designed orthogonal curve grid, which takes into account the physical, chemical and biological processes of the simulated substances and can Simulate hundreds of substances including salinity, chloride, temperature, suspended matter, various nutrients (nitrogen, phosphorus), organic matter, DO, pH, heavy metals, microorganisms and more. Water quality files can be designed in the process library PLCT (Deltares, 2020). The water quality module is widely used for the simulation of sand transport, wave patterns, topographic evolution, water quality and water ecology in the ocean, rivers, waterways, coastal ports and other areas.

Control equation and calculation method

The Delft3D-WAQ module contains 11 sets of state variables, which can be set to 543 water quality processes and their associated parameters and is used to simulate the various migration transformations of solutes in the water column. The core problem of the water quality model is to solve the convection-diffusion-reaction equation, the essence of which is the conservation of mass of substances.

$$\frac{\partial M}{\partial t} = advection + dispersion + source$$

That is, the change in mass with time is the sum of the convective, diffusive and source terms. The final three-dimensional expression for the convection-diffusion-reaction equation is:

$$\frac{\partial C}{\partial t} + v_x \frac{\partial C}{\partial x} - D_x \frac{\partial^2 C}{\partial x^2} + v_y \frac{\partial C}{\partial y} - D_y \frac{\partial^2 C}{\partial y^2} + v_z \frac{\partial C}{\partial z} - D_z \frac{\partial^2 C}{\partial z^2} = \mathrm{S} + f_R(C,t) \qquad (7)$$

with,

C	the concentration[g/m^3],
v	the flow rate[m/s],
D	the diffusion coefficient[m^2/s],
S	the inflow term,
f_R	the reaction term.

The hydrodynamic model is the basis for the construction of the water quality model, which provides the flow field conditions for solving the convective diffusion equations. Compared to the hydrodynamic model, the grid of the water quality model does not require high spatial and time step requirements, and the grid can be appropriately aggregated during the simulation to improve computational efficiency. However, the information in the hydrodynamic file includes flow field conditions, vertical mixing and diffusion terms, so care should be taken in the aggregation process to prevent the loss of local advection and diffusion information.

4.2 Model set-up

Delft3D-FLOW was used to do hydrodynamic modelling, which produced estimations of the water level and flow velocity. The water quality modelling suite of Delft3D software, Delft3D-WAQ, was used for the modelling of water quality. Here, the pertinent state-variables (substances in Delft3D-WAQ) and physical, biological, and chemical processes that affect the water quality of coastal rivers and estuaries were chosen. Through the coupling process, the outcomes of the hydrodynamic model were considered in the water quality model.

4.2.1 Hydrodynamic modelling

The FLOW module of the Delft3D software was used to carry out the numerical modelling of the hydrodynamics of Yong River. The hydrodynamic model is the basis for water quality modelling, which provides advection, diffusion, vertical mixing for the water quality model. Therefore, to simulate water quality well, it is first necessary to ensure that the hydrodynamic simulation results are accurate. Before building the hydrodynamic model, it is necessary to prepare the input information required for the model, including underwater topography, water level, tide level and other measured information. In Chapter 3, the required and source of data was provided. The follow will introduce the hydrodynamic model modelling progress.

4.2.1.1 Make the boundary file for the calculated area

The purpose of boundary extraction is to design grids for reference. The boundary can be obtained by finding the location of the Yong River on Google Earth and outlining the land and sea boundary of the Yong River and its estuary area by manually tracing the line. The document with boundary in the .kml file can be derived. Then according to Delft3D boundary file requirements, the .kml file is converted to a .ldb file, to obtain the computational boundary for Delft3D reference, as shown in the Figure 6.

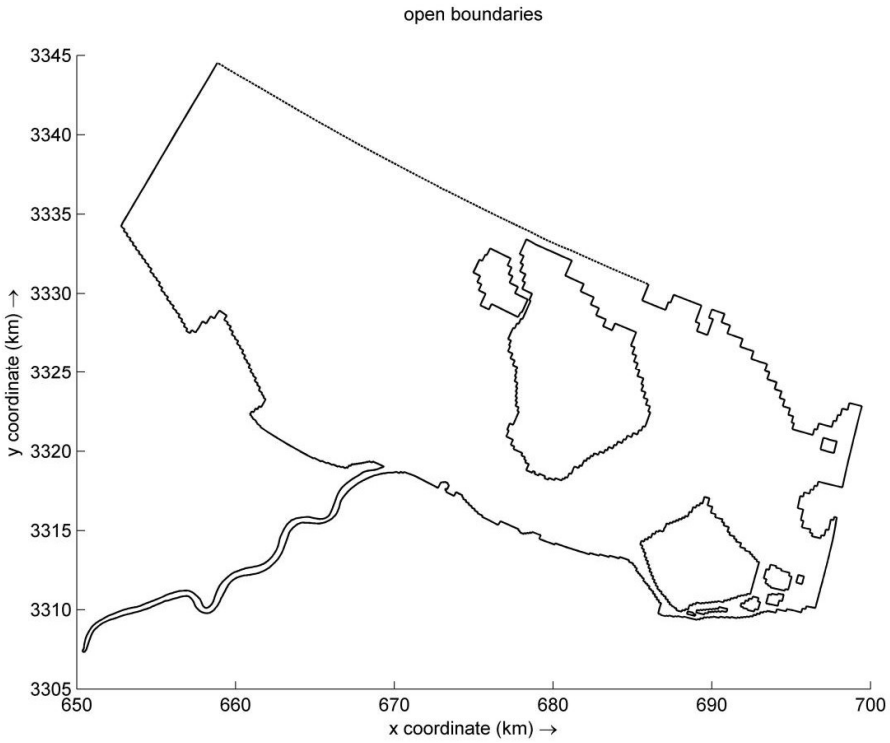

Figure 6. Yong River Estuary Coastal Boundary.

4.2.1.2 Hydrodynamic grid and bathymetry

The Yong River and the surrounding marine area are represented in Delft3D by the hydrodynamic grid. The study domain, which is roughly 49x18 km and is located near the Yong River Estuarine area, was chosen to address the goals of this research. By using such a broad spatial coverage, it is possible to prevent computational instabilities and undesirable boundary effects from happening when the boundary conditions are too close to the area of interest.

(a) Grid meshing

The quality of the computational grid is the key to the accuracy of the model calculation results. The Delft3D-RGFGrid utility creates the computational grid that is used by the program. Given that Delft3D cannot theoretically fill the boundary fully, the shape of the grid should be chosen in accordance with the direction of the water flow and the shape of the boundary. When dealing with challenging terrain, it is straightforward to construct a grid of zigzags at the boundary. However, it is best to avoid this situation, which will reduce computing efficiency. Since the estuary area of the Yong River has a complicated boundary made up of numerous islands and reefs, the grid should follow the aforementioned two requirements as closely as is practical.

In this study, we first load the Yong River boundary file (.ldb) and the surrounding sea area onto the Delft3D-RGFGRID, and then we build the grid boundary lines in accordance with the topographic boundary and the current direction using Spline curves.

To fill in the largely empty grid in the marine portion of the boundary, the grid density is altered after it has been generated, and the grid on the land beyond the boundary is erased. Editorial changes, such as eliminating the larger islands from the grid and considering them as solid wall borders, were made in the case of islands with significant topographic fluctuations within the computation area to prevent dispersion of the model results. Lastly, make sure the two grids are still orthogonal to one another by examining their orthogonality and smoothness.

The final computational grid is shown in the Figure 7. The longest side of the river grid is about 105m and the shortest is about 5m, the longest side of the sea grid near the estuary is about 600m and the shortest is about 50m, the total number of grids is 642×360. An orthogonality check for the grid is included with the Delft3D-RGFGRID tool. The developed computational mesh essentially satisfies the requirements and can be utilized for model calculation after being checked for orthogonality of the final grid.

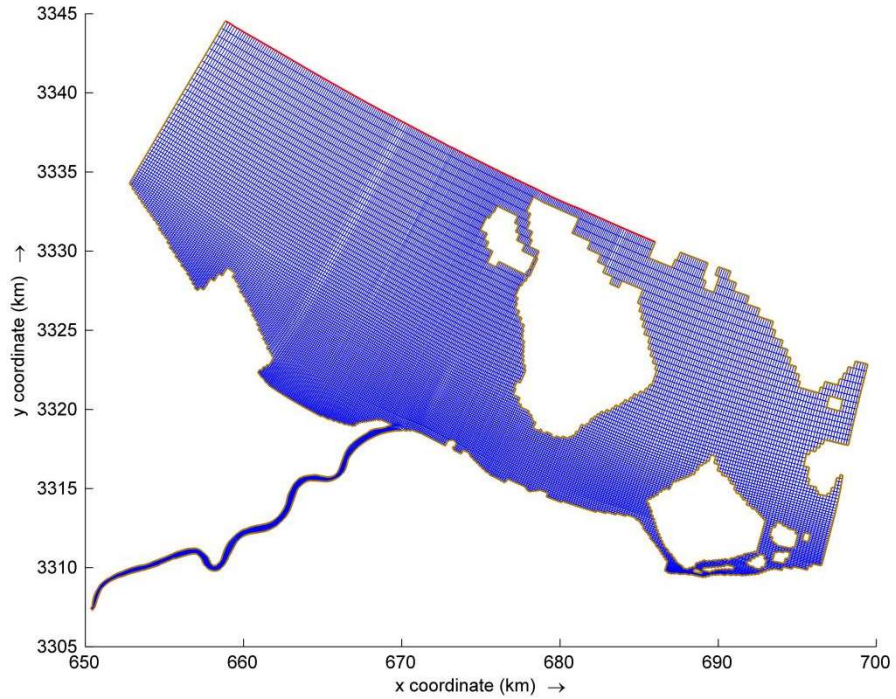

Figure 7. Model grid generated for the Yong River Estuary and the open (in red) and close (in brown) boundaries of the domain.

(b) Generation of underwater terrain

The correctness of the undersea topographical structure is one of the main elements determining the accuracy of the hydrodynamic model simulation, along with the quality of the computational grid design. China Navy Hydrographic maps are used to extract the bathymetric topographic data for this work, and the extracted elevation topographic data is modified into an .xyz file. The built grid file is entered while the .xyz file is imported into Delft3D-QUICKIN, and the underwater topography is then interpolated.

While the designed spatially discrete meshes are loading, import the edited water depth samples into Delft3D-QUICKIN. It's crucial to pay attention to the methods used while

utilizing interpolation to build underwater terrain. There are two forms of interpolation employed by Delft3D-QUIKIN: triangular interpolation and linear interpolation. Linear interpolation works best when the water depth point is dense, while triangular interpolation works best when the water depth point is sparse. In this study, triangular interpolation was chosen to make the resulting bathymetric topography more accurate. The internal diffusion was finally activated in order to provide each grid point a value based on topographic information.

The underwater topography interpolation result of the Yong River and its estuary area is shown in the Figure 8. The interpolation output indicates that the average depth of the underwater terrain for 4 to 5 meters, the depth of 114 meters. The estuary to the coast gradually deepened means that the terrain changes are consistent with a real situation. The export file terrain .dep files can be used for model calculations.

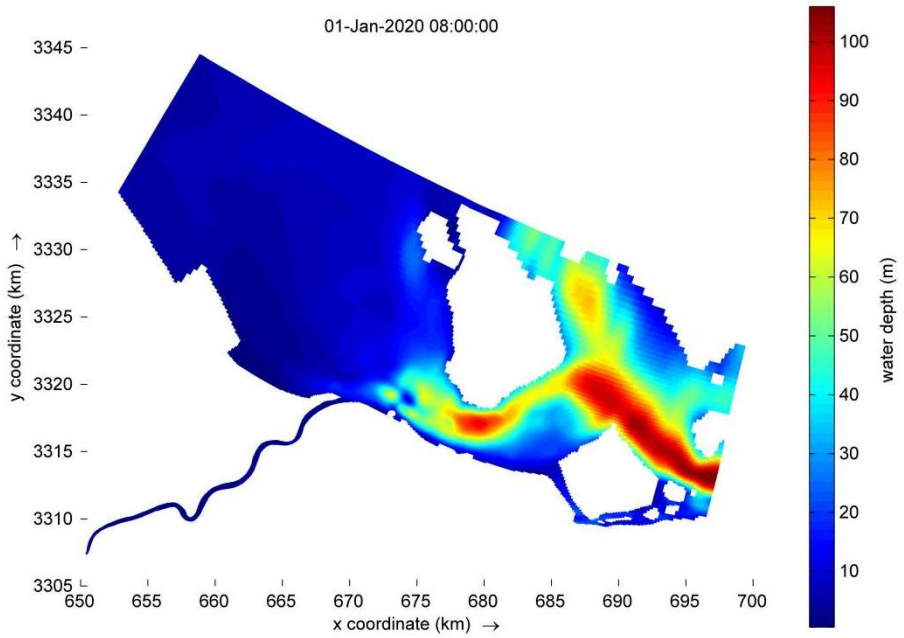

Figure 8. The underwater topography interpolation result of the Yong River and its estuary area.

4.2.1.3 Hydrodynamic model set-up

Once the mesh file and bathymetry file have been created, the hydrodynamic model is built using the Delft3D-Flow module. The GUI interface of Delft3D-Flow is shown in the Figure 9.

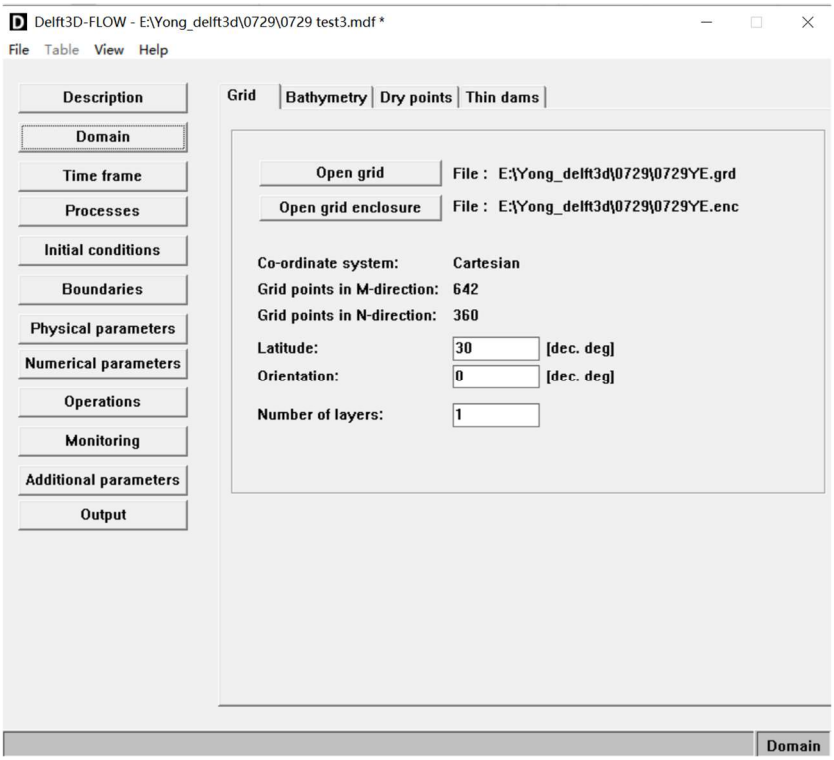

Figure 9. Delft3D-FLOW Graphical User Interface.

Domain Input grid file, the bathymetry file, the default Cartesian coordinate system, and the latitude of the Yong River is 30 dec.deg. The hydrodynamic model of the Yong River and the surrounding sea is a two-dimensional model with 1 layer of vertical stratification.

Time frame Set the start and end times of the model. The reference date is used to set the start time of the axis of the modelling results, i.e., the reference time axis. Hydrodynamic modelling was carried out for the period 1 January 2020 till 31 December 2021. The setting of the time step is crucial to the accuracy and stability of the model calculation. The Delft3D model uses the ADI alternating implicit solution method, which does not require very strict time steps, and the Delft3D-Flow manual states that the time step limit should only be kept below the Courant number of 10. However, in order to ensure the stability of the model, it is generally recommended to keep the Courant number below 1. After repeated trials, the time step was adjusted to 0.1 min to ensure the speed, accuracy and stability of the model.

Process This column is for the physical factors considered in the hydrodynamic model, where it can be set to include simulation factors such as Salinity, Temperature, Pollutants and tracers, Sediments. Physical influences such as wind, waves and the simulation of man-made pontoons (Dredging and dumping) can be added. The effect of other factors is not considered here.

Initial Conditions This column is for setting the initial variables of the model, that is, the initial conditions of the model at the beginning. Delft3D's hydrodynamic model

can choose two starting methods, namely cold start and hot start. In the case that the initial conditions are not known, the initial conditions are manually set to cold start, and the simulation results after the cold start run are used to set the initial conditions for the hot start. In this study, the cold start method was chosen and the initial conditions was set to a uniform value, water level (water level) 0m.

Boundaries This column sets the open boundary conditions for the model, which has two open boundaries for the upper river and the open sea boundary (Figure 7). The open boundary condition for the upper river is the time series water level (Figure 10). The open sea boundary conditions are calculated from the tidal reconciliation constants based on the split tides (Table 3). Due to the large amount of data, it is cumbersome to enter a large amount of data in the interface. The time series water level data can be edited into a (.bct) file format according to the model format requirements and loaded into the Boundaries section.

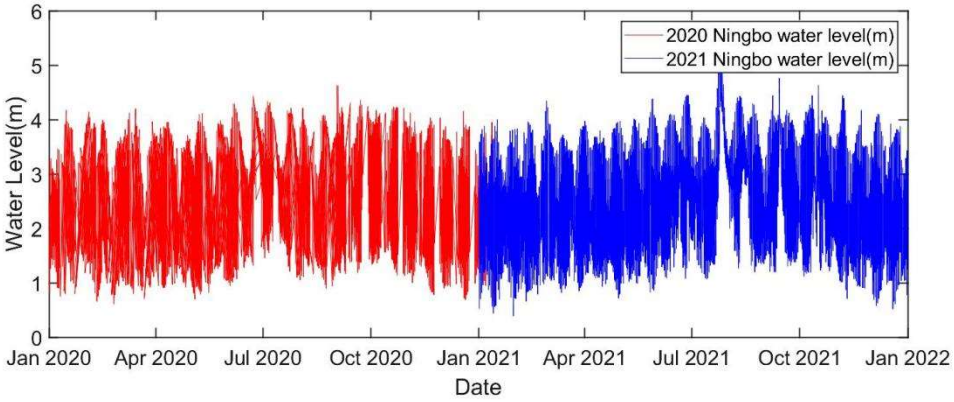

Figure 10. Time series of the water levels from the Ningbo hydrological monitoring station applied as upper open boundary conditions in the model.

Physical parameters This column is for setting the physical parameters of the model, which are key parameters for the hydrodynamic simulation and are important for the accuracy of the simulation results. The acceleration of gravity is set to 9.81m/s^2 and the density of the water column is set to 1000kg/m^3. The bottom roughness is calculated using Manning's formula and the roughness value is taken as the mean value of 0.05. The horizontal eddy viscosity is set to 10 m^2/s.

Numerical parameters This column requires the numerical parameters for the model's own solution to be set, where the default values for the model are generally taken.

Operations Set the closed boundary of the model, i.e., the location of the model's inlet and the flow rate.

Monitoring This column sets the location of the monitoring points in the model. The Delft3D hydrodynamic model will keep a complete history of the monitoring

points for comparison with the actual monitoring values, so the location of the actual monitoring stations needs to be set here. The simulation has one river level monitoring station and four tidal level monitoring stations. The river level monitoring station is Wangjiayang (WL01). The tidal stations are Zhenhai station (WL02), Jintang tidal station (WL03), Xiasanshan tidal station (WL04) and Dinghai station (WL05). The corresponding grid positions were found according to the actual locations of the monitoring stations. The final open and closed boundaries and the locations of the monitoring points are shown in the Figure 11.

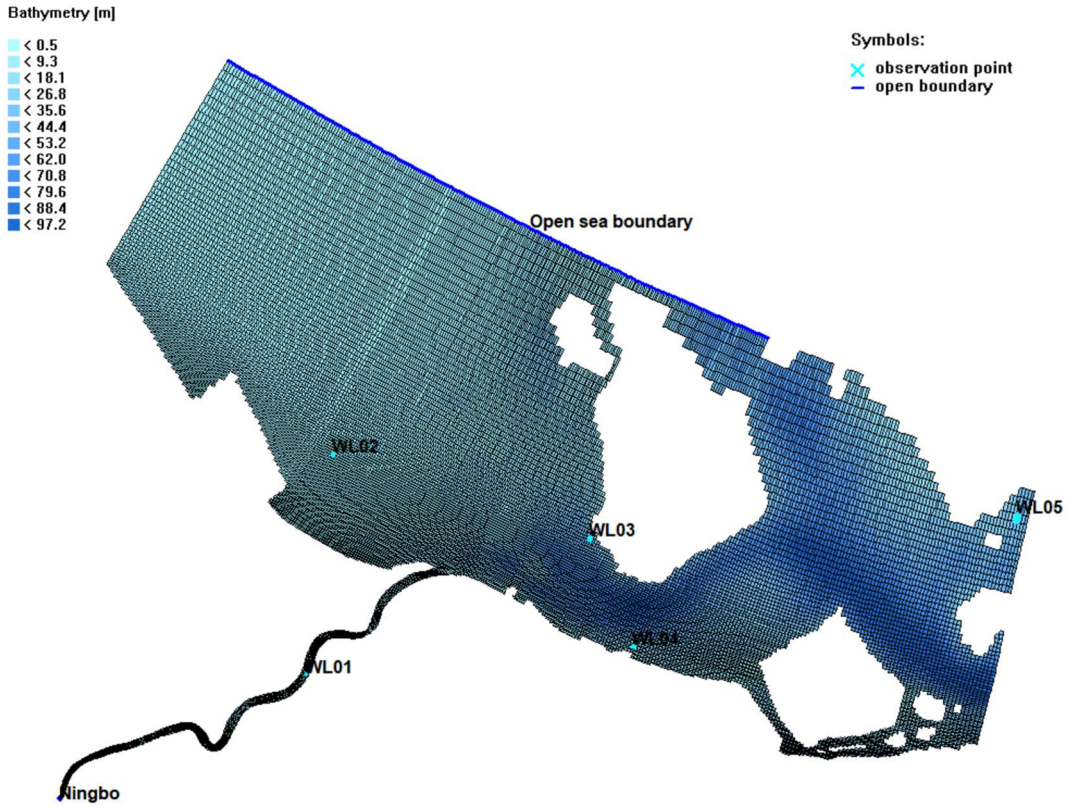

Figure 11. The location of five monitoring points and two open boundaries.

4.2.1.4 Calibration of hydrodynamic model

Model calibration is a key part of the modelling process, enabling the model to be applied to the calculation of water movement in the region. The main operation of the model rate is to adjust the parameters appropriately. The calibration entails adjusting the Manning friction coefficient to reproduce the observed signals of the water levels at the various tidal stations. The model was rate calibrated using field observations from January 2020 to April 2021. The model simulation and actual observations were compared to determine whether the model calibration and validation results met the accuracy requirements (Figure 12).

The performance of the model is assessed with the coefficient of determination (R^2), the calculation formula is:

$$R^2 = 1 - \frac{\sum(y_i - \hat{y}_i)^2}{\sum(y_i - \bar{y}_i)^2} \quad (8)$$

Where y_i are the observed values of the water level, $\hat{y}_i$ are the predicted values, and $\bar{y}_i$ is the mean of the observations.

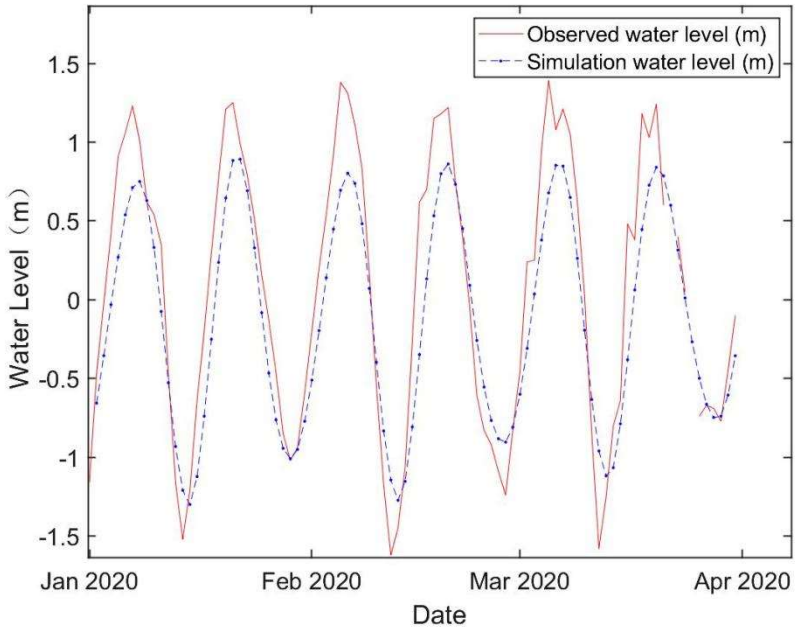

Figure 12. Daily water level fluctuation during January 2020 to April 2020 at the Zhenhai (WL02).

Table 5. Calibration results of five water level monitoring stations.

Water Level Station	R^2
Wangjiayang (WL01)	0.9638
Zhenhai (WL02)	08957
Jingtang(WL03)	0.9345
Xiasanshan (WL04)	0.9392
Dinghai (WL05)	0.6195

The sensitivity of various model configuration adjustments to the model outcome was the main focus of this study. These modifications included the adjust of model time step, the manning uniform friction coefficient, and the horizontal viscous coefficient. The coefficient of determination of the results are shown in the Table 5. From the Table 5, the water level and water validation graphs at the monitoring stations work well, and the final selection:

Time step = 0.1 min

Manning uniform friction coefficient = 0.05

Uniform horizontal eddy viscosity = 10 m^2 /s

Table 6. Hydrodynamic Model parameter values summary table.

Name of Parameters	values
Co-ordinate system	cartesian
Grid points in M-direction and N-direction	642×360
Latitude	30°
Number of layers	1
Reference date	January 1st, 2019
Simulation strat time	January 1st, 2020 8:00
Simulation stop time	December 31, 2021 22:00
Time step	0.1 min
Gravity	9.81 m/s^2
Water density	1000kg/m^3
Manning roughness	0.05
Horizontal eddy viscosity	10 m^2/s

4.2.2 Water quality modelling

The Delft3D-WAQ module is used to build the water quality model. The input files for the Delft3D-WAQ module must be prepared in advance, just like with the hydrodynamic model. The first is the coupling of the hydrodynamic simulation results to supply the flow field for the water quality model and to test the stability of the coupled flow field to ensure the mass conservation during the water quality simulation. The second is the coupling of the hydrodynamic simulation results to the water quality model. The fundamental procedures for water quality modelling are:

(1) Take the outcome of the hydrodynamic simulation and adjust it so that it can be used in the water quality simulation.

(2) Define the components and water quality procedures you intend to use.

(3) Utilizing the results of the first and second steps, define the water quality simulation in this step. You will need to define the simulation time, waste loads, initial conditions, boundary conditions, output variables, etc.

(4) Start the simulation.

(5) Examine the results.

Depending on what one wants to alter, one can either be ready after step 5 or go back to steps 1, 2, or 3. Steps 3 through 5 are frequently repeated.

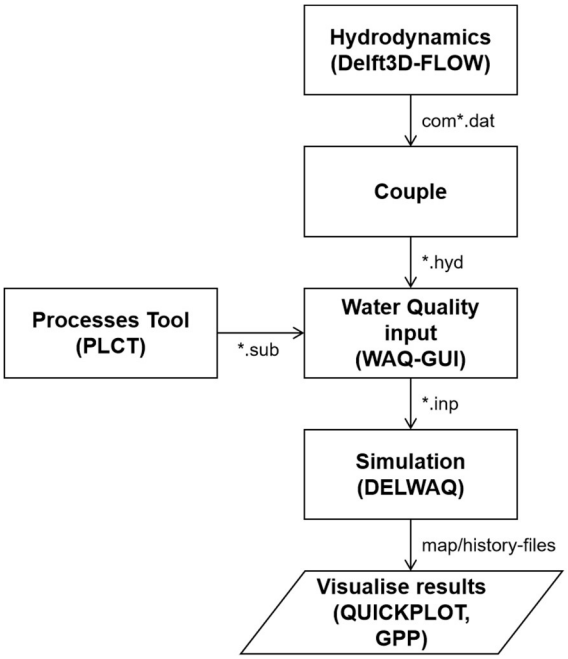

Figure 13. The fundamental modules of water quality modelling with data flow.

D-Water Quality offers a lot of flexibility in its water quality modelling. For example, the substances, water quality processes, output variable can be freedom selected. The water quality module's Processes Library is used to choose the materials and procedures that will be represented. A wide range of water quality criteria are covered by the extensive collection of substances and processes in the Processes Library. Deltares plans to make premade sets available to make it easier to choose elements and procedures quickly for a particular type of model, such as a model for eutrophication or a model for dissolved oxygen. The user interface of Delft3D allows for choices.

A great variety of physical, (bio)chemical, and biological processes in D-Water Quality can be specified. Any group of substances and processes can be chosen from the processes that are stored in the so-called Process Library. Select the water quality parameters and set the water body components and physicochemical processes that the water quality model will simulate under the Delft3D-Process Library Configuration Tool. This is a crucial phase in the water quality model since, even in a detailed eco-dynamic model, it is unrealistic to mimic all the physico-chemical processes that take place in a water body, and many of the mathematical equations related to these processes are still of an empirical character. Many of the water quality characteristics that must be included into the formulas are difficult to determine by practice and are frequently adjusted based on prior knowledge and the accuracy of simulation results, which is challenging for the current study. As a result, it is required to highlight the emphasis of the simulation, create a simple and reliable water quality model, and suitably simplify the water quality processes in the water body.

4.2.2.1 Water quality processes and formulations

The water quality model framework was constructed according to the actual situation of Yong River and its estuary. The simulation of water quality mainly focuses on the simulation of dissolved oxygen in the water body. Combined with the measured data, the simulated substances include DO, BOD_5, COD, NH4-N and OPO4, and the water quality processes include DO cycle, nitrogen and phosphorus cycle, the physical diffusion of substances in the water with the water migration, and the mutual biological and chemical transformation of different substances (Figure 14). The following processes were included in the water quality model for the Yong River and its estuary:

- reaeration of oxygen
- nitrification and denitrification
- mineralization of organic matter
- phosphate adsorption and precipitation

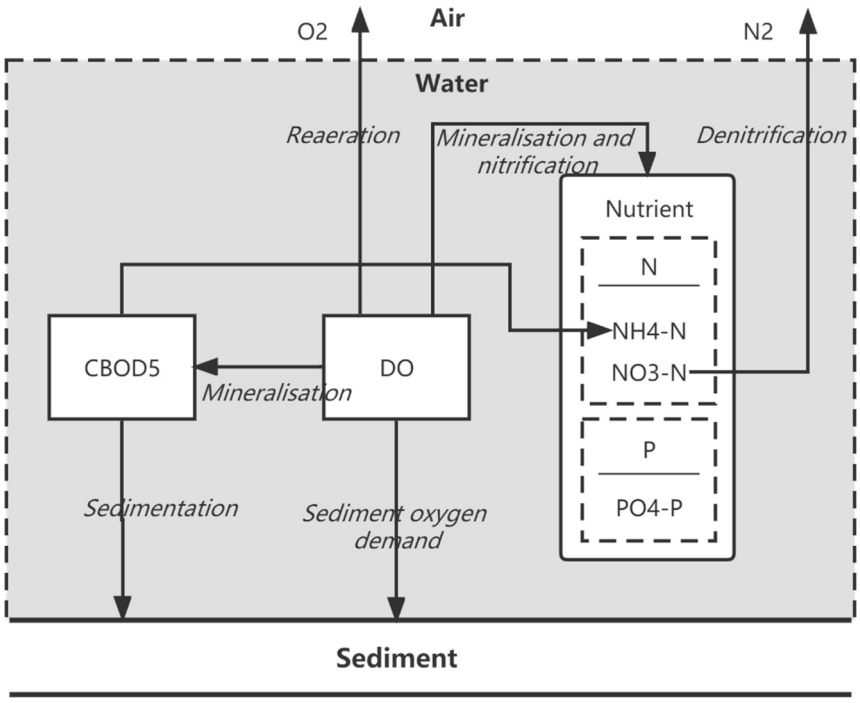

Figure 14. Relationship between substances of water quality.

DO is one of the most crucial elements affecting water quality in the water ecosystem. Most of the physical and chemical processes in water bodies involve oxygen, such as water surface reoxygenation, nitrification, mineralisation, respiration, photosynthesis, etc. Therefore, dissolved oxygen concentration is commonly used in environmental monitoring to determine the quality of regional water quality. The level of DO concentration is the result of various physico-chemical processes in the water body, which means that the level of DO concentration is basically the most direct reflection of the quality of an area's water body, and low concentrations of dissolved oxygen are often accompanied by poor water quality conditions.

To simulate the DO concentration in water quality models, there are two possible approaches. The first is to create a physical numerical model that is endlessly accurate. All water quality processes that affect DO concentration, such as phytoplankton amount, zooplankton amount, salinity, temperature, acidity and alkalinity, sediment, nitrogen, phosphorus, and other organic matter, will be accurately simulated depending on the results of the DO concentration as the final link in the water quality simulation process. The processes of nitrification, mineralization, and denitrification of organic matter are all closely related to the material cycle, so each of these influencing substances must have its own material cycle. For instance, simulating algae requires simulating inorganic salts that must match the type of organic matter. Setting parameters for the model is a challenge because a simulation of this kind requires tuning a wide range of parameters, many of which are challenging to obtain in practice. As a result, the study in this work is currently challenging. Another way of thinking is to use Streeter and Phelps' strategy. Streeter and Phelps came up with the idea of using an aggregate parameter to represent all the organic compounds, namely the biochemical oxygen demand BOD. There is a huge diversity of organic molecules in the natural water column, as well as numerous microscopic inorganic chemicals that are challenging to identify and confirm. Their degradation also affects the dissolved oxygen concentration in the water column, so Streeter and Phelps came up with the idea of using an aggregate parameter to represent all the organic compounds, namely the biochemical oxygen demand BOD. This is the basis for the simulation of dissolved oxygen in this paper.

BOD is biochemical oxygen demand (Biochemical Oxygen Demand), refers to the total amount of dissolved oxygen consumed by biological or chemical action in a certain time at a certain temperature. It is a measure of the total amount of organic matter in the water body of a water quality monitoring index. The general monitoring method is to take a sample of organic matter in the field, fill it with water and dilute it to determine the dissolved oxygen concentration, and then measure the dissolved oxygen concentration again after the sample has been left at room temperature for 5 days at 20°C. The difference between the dissolved oxygen concentration before and after is the amount of dissolved oxygen consumed by the degradation of the organic matter at 20°C for these 5 days, generally known as BOD_5, and BOD_{20} is the difference measured after 20 days. Generally, BOD refers to the biochemical oxygen demand of organic matter represented by the element carbon, BOD_5.

Reaeration

The reaeration flux at the air-water interface is proportional to the reaeration rate constant and the difference between the actual concentration in water and the saturation concentration. The value of the c reaeration flux is positive or negative depending on whether the oxygen concentration is less than or greater than the saturated oxygen concentration. The rate constant is a function of temperature, flow rate, and wind speed. The saturated oxygen concentration is a function of salinity and water temperature.
The equation of the reaeration flux as follows:

$$Flux = \frac{k}{H} \times (Oxy_{sat} - Oxy) \times \theta^{T-20} \quad (9)$$

with,

k	first order reoxygenation rate at 20° C [m/d],
H	water depth [m],
θ	temperature-dependent constant [-],
T	water temperature [℃],
Oxy	oxygen concentration [g/m^3],
Oxy_{sat}	saturated oxygen concentration [g/m^3].

The reaeration rate has been formulated as a linear function of the saturation and actual concentrations of DO as follows:

$$Rrear = klrear \times (Coxs - \max(Cox, 0.0))/H \quad (10)$$

$$klrear = l = klrear_{20} \times tcrear^{(T-20)} \quad (11)$$

$$klrear_{20} = \left(\frac{a \times v^b}{H^c}\right) + (d \times W^2) \quad (12)$$

$$Coxs = \int(T, Ccl\ or\ S\ AL) \quad (13)$$

with,

a, b, c, d	coefficients with different values for each reaeration options,
Ccl	chloride concentration [gCl/m^3],
Cox	actual dissolved oxygen concentration [gO_2/m^3],
Coxs	saturation dissolved oxygen concentration [gO_2/m^3],
H	depth of the water column [m],
klrear	reaeration transfer coefficient in water [m/d],
klrear20	reaeration transfer coefficient at reference temperature 20 ℃ [m/d],
tcrear	temperature coefficient of the transfer coefficient [-],
Rrear	reaeration rate [gO_2/m^3/d],
SAL	salinity [kg/m^3],
T	temperature [℃],
v	flow velocity [m/s],
W	wind speed at 10 m height [m/s].

Mineralization and nitrification

Both mineralization and nitrification processes are influenced by water temperature and dissolved oxygen concentration. When the water temperature drops to a certain level, the nitrification process stops, and this temperature is the critical temperature for the nitrification process. It can also be seen from the following two equations that when the dissolved oxygen concentration exceeds the optimum concentration for the mineralization process or nitrification process, the mineralization and nitrification process proceed unrestricted. When the dissolved oxygen concentration is below the critical concentration, the mineralization and nitrification process will stop completely. When the dissolved oxygen is between the critical and optimum values, it can be seen that the limiting influence of nitrification and mineralization generated by dissolved oxygen is between 0 and 1.

The mineralization process is calculated as follows:

$$Mineralization = -Rc_{BOD} \times (BOD) \times \vartheta_{BOD}^{(T-2\ )} \times \frac{(O_{20})-DO_{BOD}^{Cr}}{DO_{BOD}^{Opt}-DO_{BOD}^{Cr}} \quad (14)$$

with,

Rc_{BOD}	First order reaction rate of BOD at 20° C [1/d],
T	water temperature [℃],
DO_{BOD}^{Cr}	critical dissolved oxygen concentration for BOD mineralisation [g/m³],
DO_{BOD}^{Opt}	optimal dissolved oxygen concentration for BOD mineralisation [g/m³],
$\vartheta_{BOD}^{(T-20)}$	coefficient of influence of mineralisation temperature [-].

The reaction equation for the nitrification process of ammonia and nitrogen is as follows:

$$NH_4^+ + 2O_2 \rightarrow NO_3^- + 2H^+ + H_2O \quad (15)$$

Where the elemental mass ratio is NH_4^+：O_2：NO_3^- =-1：-4.751:1

The equation for the nitrification process is as follows:

$$Nitrification\ flux = -Rc_{nit} \times (NH_4) \times \vartheta_{nit}^{(T-20)} \times \frac{(O_{20})-DO_{nit}^{Cr}}{DO_{nit}^{Opt}-DO_{nit}^{Cr}} \quad (16)$$

with,

Rc_{nit}	First order reaction rate of BOD at 20° C [1/d],
T	Water temperature [℃],
DO_{nit}^{Cr}	critical dissolved oxygen concentration for BOD mineralisation [g/m³],
DO_{nit}^{Opt}	optimal dissolved oxygen concentration for BOD mineralisation [g/m³],
$\vartheta_{nit}^{(T-20)}$	coefficient of influence of mineralisation temperature [-].

4.2.2.2 Coupling of the hydrodynamic model to the water quality model

The Delft3D-COUPLE module first loads the com-file file produced by the hydrodynamic model in the Hydrodynamics column to symmetrize the hydrodynamic-water quality model. The com-file file is one of the output files of the Delft3D-Flow hydrodynamic model calculation results and is used to couple with other modules such as the Water Quality module and the Wave module, which hold the hydrodynamic simulation results. The coupling's start time and stop time are set to 8.00am on 1 January 2020 and 9.00pm on 31 December 2021, respectively. The start time and stop time are equal to or less than the interval determined by the hydrodynamic model. It should be noted that the time step used in this com-file file is not the same as the time step of the hydrodynamic model but is instead a separate time step used for coupling in the hydrodynamic model output file given in Delft3D-Flow, which is only used to preserve the calculation results. It may be longer than the hydrodynamic model's time step and is unrelated to the hydrodynamic model's calculation procedure. This time step must be

less than the time step in the com-file file and must be an integer multiple of the com-file file's time step. The final coupling setting is shown in Figure 15. When the coupling parameters have been set, click the Start (Start hydrodynamic coupling) button to start the coupling process. It ends when the computation is complete.

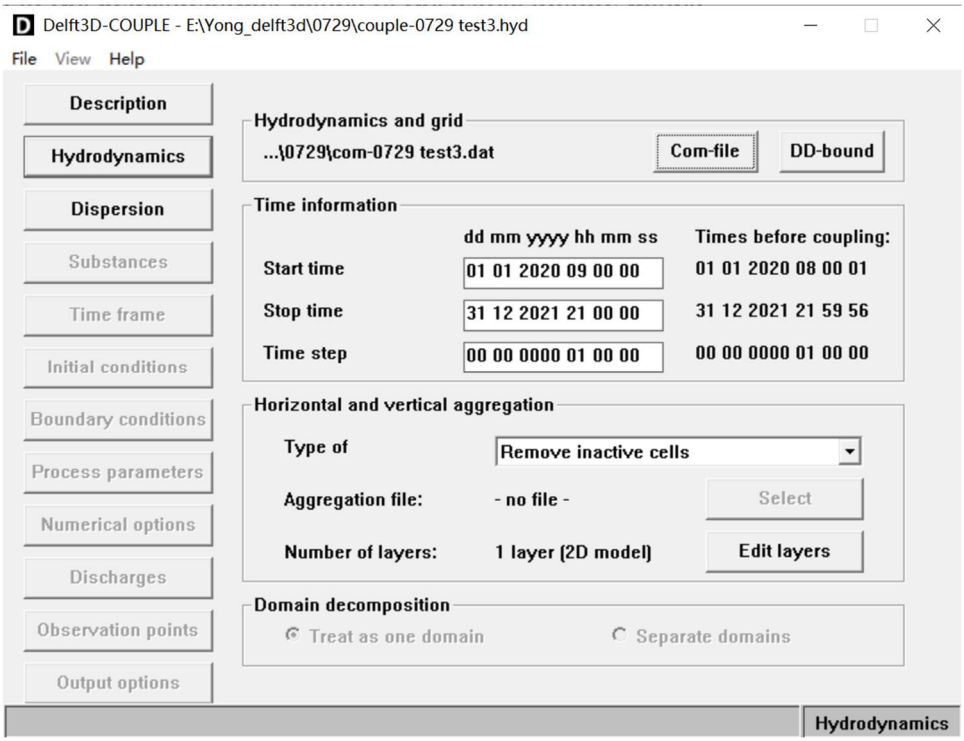

Figure 15. The settings of coupling hydrodynamic model.

4.2.2.3 Checking for mass conservation

Before developing the water quality model and include the simulated compounds, it is crucial to verify that the coupling results are accurate. The coupled hydrodynamic file might not conserve mass and might not be computationally stable because some information is lost during the aggregation process. It is crucial to verify the conservation of mass after coupling because the water quality model constructed on this foundation will undoubtedly be inaccurate.

Delft3D offers an intuitive and clever way to check the conservation of mass in hydrodynamic coupling results by offering a unique simulation substance called 'Continuity' to help test the conservation of mass in coupled files. The substance is set up in the Delft3D-Process Library Configuration Tool and has no physico-chemical significance but is simply used to test the accuracy and stability of the model. The test approach is particularly: At the open and closed boundaries, the virtual substance "Continuity" is added to all input sources with a concentration of 1 mg/L. For the beginning conditions, "Continuity" has a concentration of 1 mg/L. In practice, the coupling results are typically regarded as acceptable as long as the "Continuity" concentration stays within the range of -1 mg/L and 1 mg/L during the test. The coupling results are typically regarded as correct. Excessive variances necessitate more

investigation to determine whether the coupling procedure is flawed or whether the hydrodynamic model is accurate.

The concentration stayed within the range of 0.999 mg/L and 1.001 mg/L throughout in this study. The fluctuation range is very small, negligible, indicating that the coupling results are stable. The results of the coupling process file good, the flow field to meet the requirements of mass conservation, can be used for water quality modelling.

4.2.2.4 Water quality model set up

After completing all the above preliminary work, starting to configure the water quality model, water quality modelling under Delft3D-WAQ, click on the Define input button to start the model parameters and boundary conditions input. First load the previously coupled hydrodynamic flow field file (.hyd) file in the FLOW Module, showing the coupled time step of 1 hour. The calculation start time and end time are the first day of 2020 and the last day of 2021 respectively.

Dispersion In this column, the dispersion and diffusion coefficients of the simulated material are set, where the dispersion coefficient is 1m2/s and the vertical diffusion coefficient is 1 x 10-7m2/s. The additional vertical diffusion coefficient is chosen from the hydrodynamic simulation results.

Substance This column loads the Substance-file previously configured under the Delft3D-Process Library Configuration Tool, from the interface you can see the selected water quality process and output parameters, as shown in Figure 16.

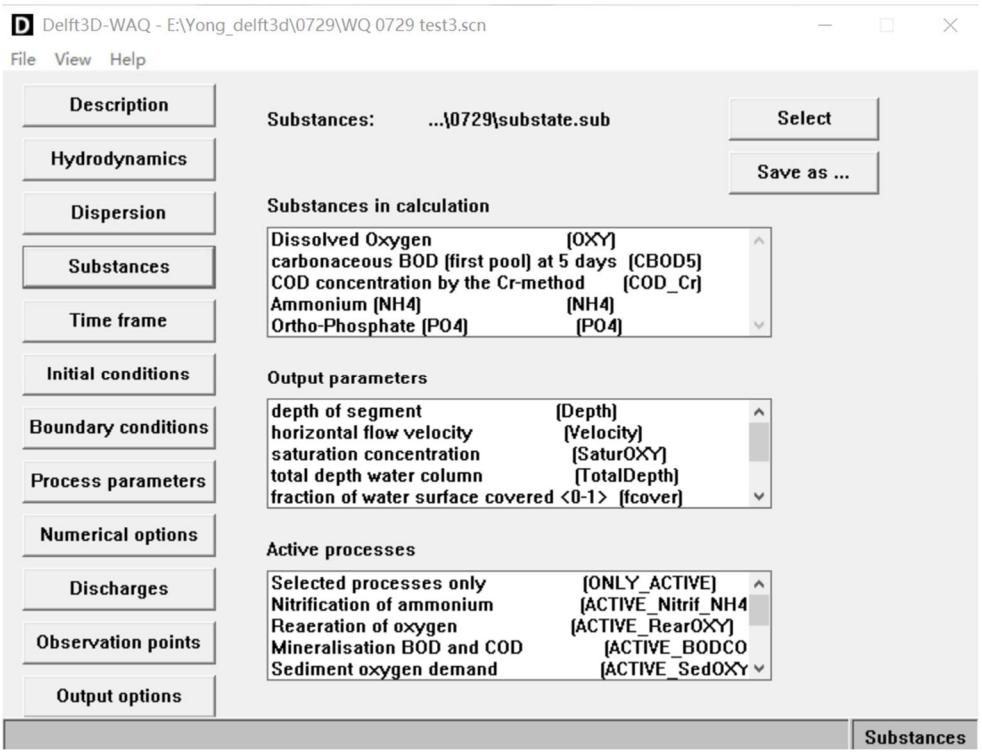

Figure 16. Water quality process and output parameters of water quality model.

Time frame This column sets the time parameters of the water quality model. It should be noted that the calculation time and termination time must be within the time range of the coupled hydrodynamic file, the time step can be greater than the time step of the coupled file. Here choose the same start and end calculation time as the hydrodynamic file, the start time is 1 January 2020 at 08:00, the end time is 31 December 2021 at 23:00, the calculation time step to take 1 hour.

Initial condition This column sets the initial variables for the modelled substances, i.e. the initial concentrations, where the initial concentrations of dissolved oxygen, biochemical oxygen demand and ammonia nitrogen in the study area need to be set. Here the average values of the monitoring data from the Yong River near sea water quality monitoring station for the years 2020-2021 are used as the initial variables, with DO at 7.845 g/m^3, BOD at 1.1125 gO_2/m^3, COD at 2.9583 gO_2/m^3, NH_4^+ at 1.0403 gN/m^3 and PO_4^{3-} at 0.047 gP/m^3.

Boundary conditions To set the open boundary conditions for the water quality section, the same open boundary location as the hydrodynamic model needs to be selected. The open boundary location is exactly at the water quality monitoring station Ningbo and ZJD12012, so the measured data from the Ningbo monitoring station and the ZJD12012 monitoring station are used here as the open boundary inputs for the upper reaches of the Yong River and the sea respectively.

Numerical options Select the numerical solution of the model, here the default 15th solution of the model is chosen, which uses the windward implicit solution.

Observation points The locations of the monitoring points are written in the Delft3D coordinate system and are located at the first and second grid points in the M and N directions. The monitoring points are Zhangjianqi (WQ02), Youshan (WQ03), ZJD02013, ZJD02018, ZJD02019 and ZJD12014, and the locations are shown in Figure 17.

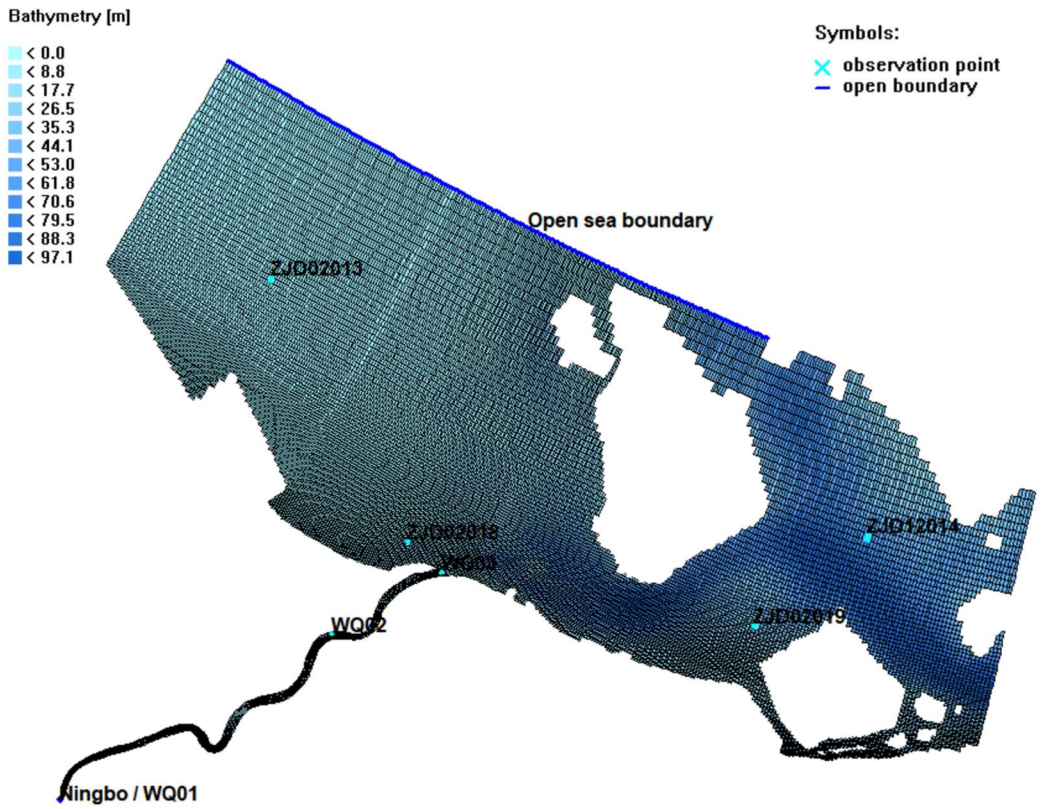

Figure 17. The location of six water quality monitoring points and two open boundaries.

Output Options There are three types of output files: the map-file, the history-file, and the Monitor-file. Each calculation unit's temporal fluctuation of the simulated material is recorded in the map-file, which demonstrates the overall variance of the simulation results. For each calculating unit, the history-file records the magnitude of the variables at a specific moment. For the model hot-start, the History-file can be utilized as a restart file. The Monitor-file is a file that keeps track of how the simulated material changes over time at the monitoring point's position. Also included are depth-averaged concentrations of the simulated compounds and the average daily change in substance concentration.

Once the input file has been generated, pre-process the file by clicking on Waq (1) to load the generated input file. Complete the pre-processing and start running the model when prompted with no errors, click on Waq (2) to automatically run the pre-processed file and wait for the simulation results.

4.3 Methods of model verification

The performance of the model is assessed with the Root-Mean-Square Error (RMSE) and the Nash-Sutcliffe Efficiency Coefficient (NSE). The former indicates whether the trend of the measurements is captured, and the latter provides an idea of the accuracy of the model.

$$\mathrm{RMSE} = \sqrt{\frac{1}{\mathrm{n}}\sum_{i=1}^{n}(\mathrm{x}_\mathrm{i}^{\mathrm{sim}} - \mathrm{x}_\mathrm{i}^{\mathrm{obs}})^2} \quad (17)$$

$$\mathrm{NSE} = 1 - \left[\frac{\sum_{i=1}^{n}(\mathrm{x}_\mathrm{i}^{\mathrm{obs}} - \mathrm{x}_\mathrm{i}^{\mathrm{sim}})^2}{\sum_{i=1}^{n}(\mathrm{x}_\mathrm{i}^{\mathrm{obs}} - \mathrm{x}_\mathrm{i}^{\mathrm{mean}})^2}\right] \quad (18)$$

where $\mathrm{x}_\mathrm{i}^{\mathrm{obs}}$ are the observed values, $\mathrm{x}_\mathrm{i}^{\mathrm{sim}}$ are the simulated values, and $\mathrm{x}_\mathrm{i}^{\mathrm{mean}}$ is the mean of the observations.

.

The root mean square error (RMSE) is a measurement of the typical error between the model and observations in the units of the quantities evaluated. A skill of 1 indicates complete agreement and a skill of 0 indicates that the model is comparable to the mean of the observations. Skill is a unitless measure of the relative average error between the model and observations.

The NSE is a model quality evaluation metric that is typically used to confirm the accuracy of the hydrological model simulation results. NSE ranges in value from -infinity to 1. The model is credible if NSE is close to 1, the model quality is good, and the simulated findings are reasonably close to the observed data' mean levels, i.e., the majority of the results are reliable, but the process simulation error is significant, and the model is not credible if NSE is significantly less than 0.

5. Results

5.1 Water level variations

The water level data validation data was selected from hourly water level monitoring data for 2020 and 2021 at five points provided by the Zhejiang Water and Rainfall Monitoring and Warning Platform of the Zhejiang Hydrological Management Centre (ZJHMC) and the Rainfall Information System of the Ningbo Water Resources Bureau (NBWRB). Figure 18 displays the variations in water levels at water level monitoring station (Wangjiayang WL01) in the river channel and Figure 19 shows those at the four additional stations (Zhenhai WL02, Jintang WL03, Xiasanshan WL04, and Dinghai WL05) in the sea close to the Yong River Estuary. The obtained and real observation graphs were compared, with measured values in red and simulated values in blue.

As can be seen from the water level comparison results (Figure 18 and Figure 19), the simulated values better reflect the measured conditions. The observed water level at the river channel water level monitoring station WL01 ranges from -0.9m to 2.31m (Figure 18). The river channel's water level varies throughout the year, being lowest from April to June, with a minimum value of -0.90m, and highest from July to November, with a maximum value of 2.31m. There are noticeable seasonal variations in the water level. The water levels in the river channel were slightly higher in the simulation than they were in reality.

The sea area experiences slightly different water level fluctuations than the river channel, with the lowest water levels typically happening in January through March and the greatest levels typically occurring in April through May. (Figure 19). The observed water levels of the four open sea water level monitoring stations exhibit almost the same trend throughout the course of the year. At the four open sea area stations, the simulated water level values are similar to the observed. The simulated water levels are more similar to the observed values the farther from the estuary and the shore (The distance from WL02 to WL05 to the mouth of the river and the coast is getting farther and farther.). In the open sea area, the simulated water levels being slightly smaller than the observed water levels.

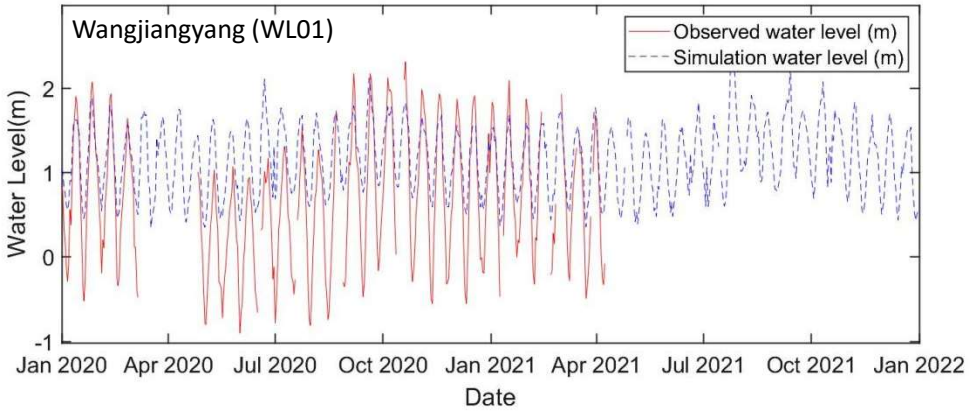

Figure 18. Daily water level fluctuation during 2020 and 2021 at the river channel. The water level monitoring station is Wangjiayang (WL01).

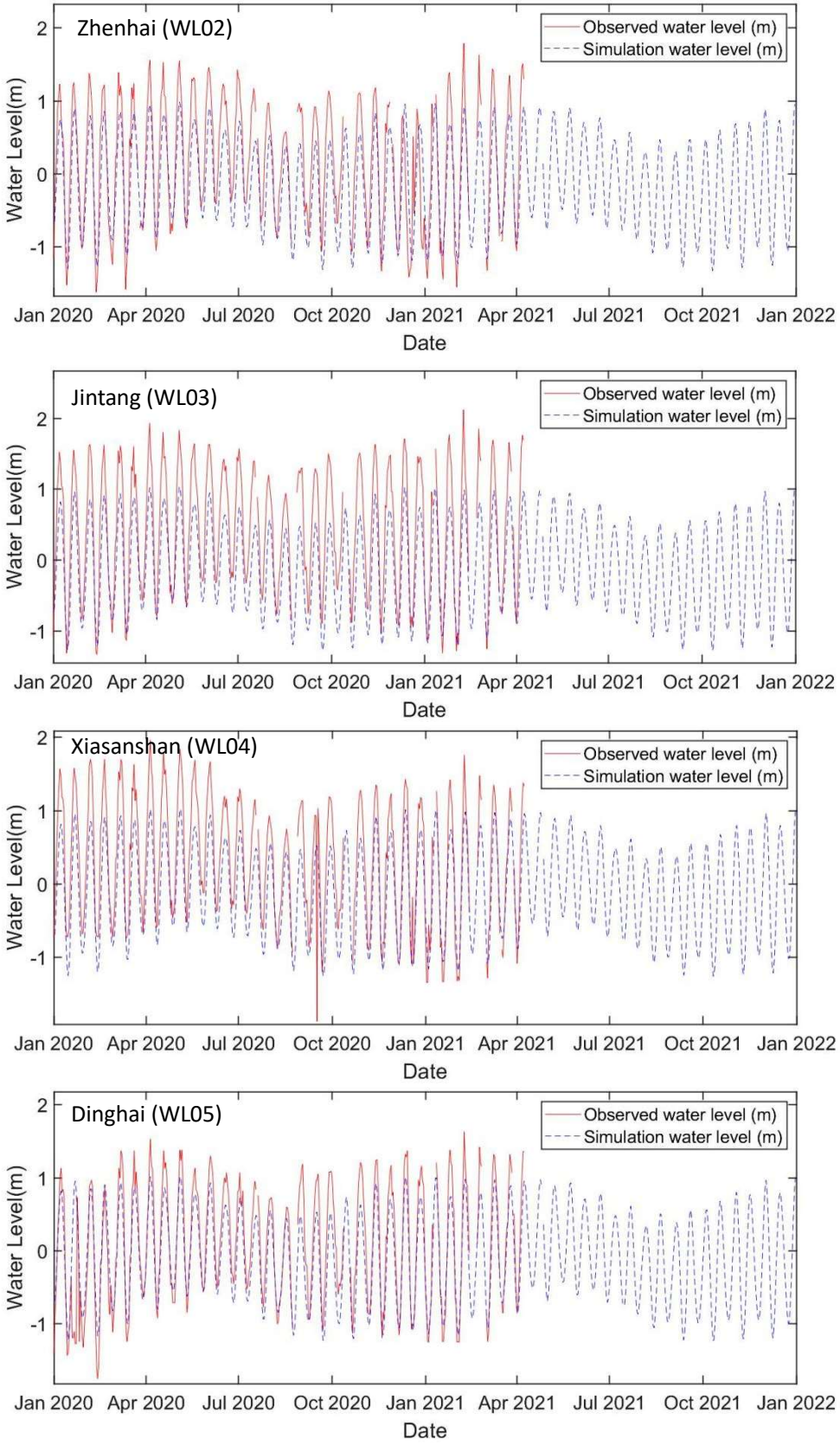

Figure 19. Daily water level fluctuation during 2020 and 2021 at the estuary and the open sea area. The four water level monitoring stations are Zhenhai (WL02), Jintang (WL03), Xiasanshan (WL04), and Dinghai (WL05).

Table 7. Statistical parameters used to assess the quality of the water levels calculated by the two-dimensional hydrodynamic model. Ideal values: $R^2 > 0.7$; RMSE: 0; NSE: Excellent (→1), Reasonable (→0), Poor (→-∞).

Water Level Station	R^2	RMSE	NSE
Wangjiayang (WL01)	0.7370	0.2090	0.2711
Zhenhai (WL02)	0.7397	0.3193	0.5857
Jingtang(WL03)	0.9021	0.1989	0.4338
Xiasanshan (WL04)	0.8360	0.2538	0.5988
Dinghai (WL05)	0.9213	0.1737	0.7908

The R^2 between the simulated and real values of the water levels ranged from 0.73 to 0.93. The large planar computation grid of the hydrodynamic model created in this research, which has some divergence in space between the grid where the monitoring points are located and the actual location, may have contributed to the mistake in part. The modelled water level simulations are near to the mean of the actual values, as shown by the fact that the minimum and maximum RMSE values for the five sites are both reasonably close to zero (0.1737 and 0.3193). The NSE of the observed points progressively rises and approaches 1 from the river to the outer sea, demonstrating the model's plausibility and the accuracy of the simulated values.

5.2 Water quality variations

Figure 20 gives a comparison of the measured and simulated values of Dissolved oxygen concentration (DO), Chemical oxygen demand (COD), Ammonium concentration (NH_4^+), and Ortho-Phosphate concentration (PO_4^{3-}) at 3 water qualty monitoring stations in the river channel, estuary, and open sea areas respectively. The observed values in red and simulated values in blue.

The water quality parameter concentrations exhibit seasonal variations as well, as can be seen from the monthly average of the water quality observed data and the simulation values comparison chart (Figure 20). The majority of water quality parameter concentrations follow the same trend in the river channel and estuary as they do in the open sea areas. The concentrations of all water quality parameters in the outer sea are significantly lower than those at the water quality monitoring stations in the river channel and estuary.

The simulation results of each water quality parameter in the river channel and estuary are basically consistent with the measured results, and the change trend is more consistent with the measured results. For example, the simulation value of DO concentration in the river channel and estuary is more in line with the measured values

(Figure 20 (a)). In the open sea areas, the simulated results of water quality parameters show some deviation, the further away from the estuary, the greater the deviation between the simulated and measured values of water quality parameters, such as the NH_4^+ concentration and PO_4^{3-} concentration at water quality monitoring station ZJD12014 (Figure 20 (c) and Figure 20 (d)).

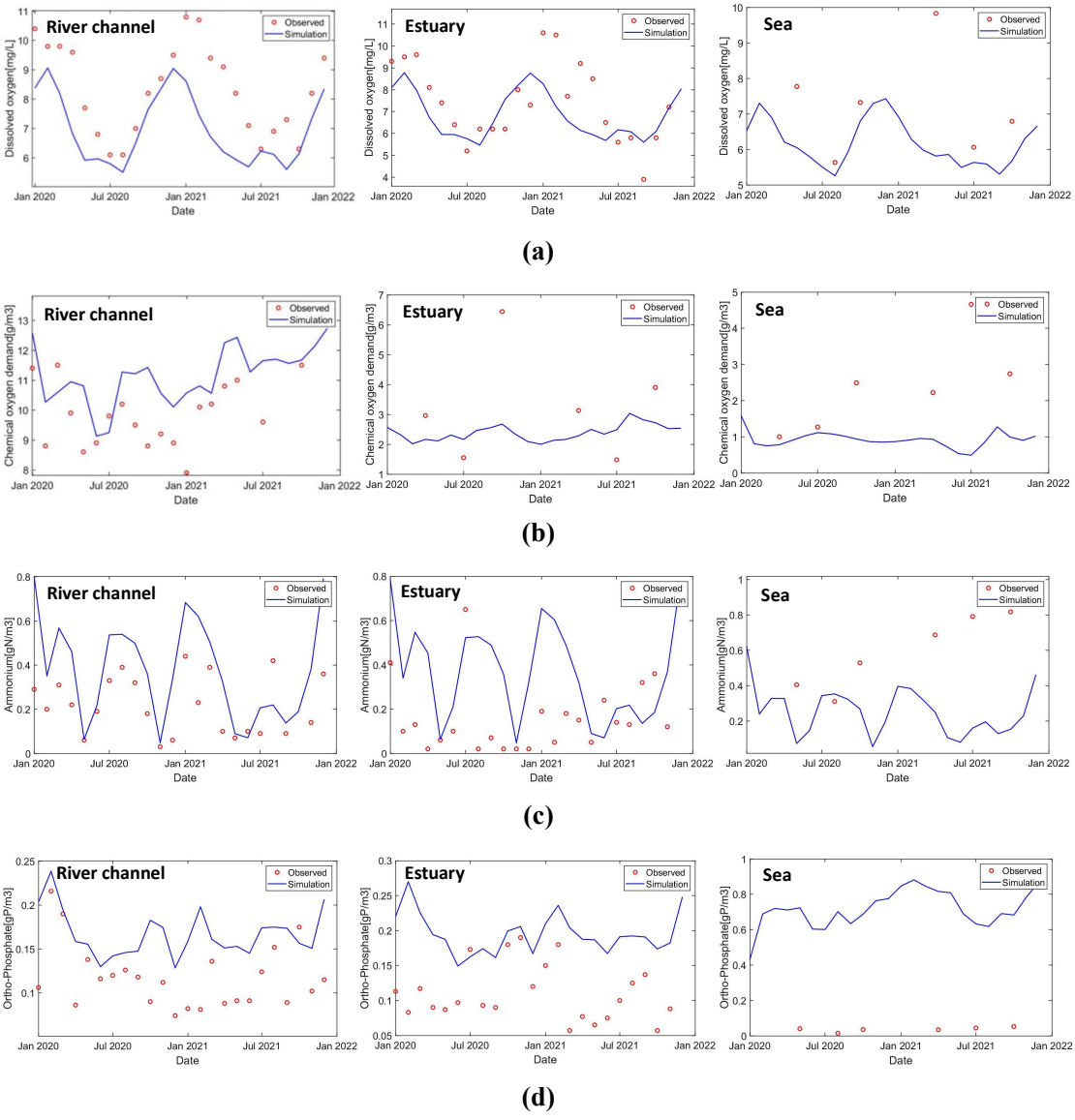

Figure 20. Water quality parameters concentration at the Yong River's river channel, estuary, and open sea areas. (a) Dissolved oxygen concentration, (b) Chemical oxygen demand, (c) Ammonium concentration, (d) Ortho-Phosphate concentration.

The model simulation results for error analysis are based on the water quality simulation results of each monitoring station and the comparison of measurement data (Table 8). While the average relative error of the remaining water quality indicators is less than 33% and the lowest relative error of DO is 11%, the average relative error of the indicators NH_4^+ and PO_4^{3-} is rather high. The observed value of the water quality indicators is typically lower at water quality monitoring points than the simulated value, as can be seen from the monthly average of the water quality observed data and the

simulation values comparison chart as well. The fact that the simulation process in this thesis only takes into account the influence of nutrients, rather than other potentially relevant factors like heavy metals, organic matter, and oil, as well as potential influences from rainfall and other factors, may be the cause of the high average relative error of NH_4^+ and PO_4^{3-}. In general, the error level is within acceptable bounds, and the water quality model developed in this study can capture the trends of water quality variables well.

Table 8. NSE of water quality result.

Water Quality Station	DO	COD	NH_4^+	PO_4^{3-}
Zhangjianqi (WQ02)	-0.1817	0.8977	-1.3713	-1.8409
Youshan (WQ03)	0.5835	/	-2.7235	-3.1688
ZJD02013	0.9603	0.7142	-0.0416	-
ZJD02018	0.8996	0.2957	0.1745	-
ZJD02019	0.9241	0.2850	0.2954	-
ZJD12014	0.9151	-	0.3251	-

Seasonal differences will have an impact on the tidal conditions and freshwater inflow, which will subsequently have an impact on the hydrodynamic circulation and the values and distribution of water quality parameter concentrations. The Yong River basin has a dry season runs from November to March, followed by a complete water season from April to October. June is the flood season and January is the dry season.

With pronounced seasonal fluctuations, DO concentrations in the river channel and the vicinity of the estuary were lower in July throughout the summer and higher in spring and fall (Figure 20 (a) and Figure 21). (The variation in DO concentration in the sea area near the open boundary does not accurately reflect the actual situation since the model is affected by boundary conditions, so we will not consider here.) According to Figure 22, BOD has a consistent seasonal distribution with greater values in the summer and winter, showing organic pollution in the harbour at the estuarine area. COD clearly varies seasonally as well, with winter having the highest COD at the river channel (Figure 20 (b) and Figure 23). In the waters surrounding the estuary, COD is higher along the shoreline, especially on the western side of the estuary which has a significantly higher COD in winter. Higher amounts of NH_4^+ in the river channel occurred in winter than those in spring and summer (Figure 20 (c) and Figure 24). In winter, NH_4^+ advected around the estuary, and the value in this area are also noticeably higher than in other zones of sea. This may be due to the reduced freshwater inflow from the river to the ocean during the dry season in January, which allows pollutants to accumulate in the estuary.

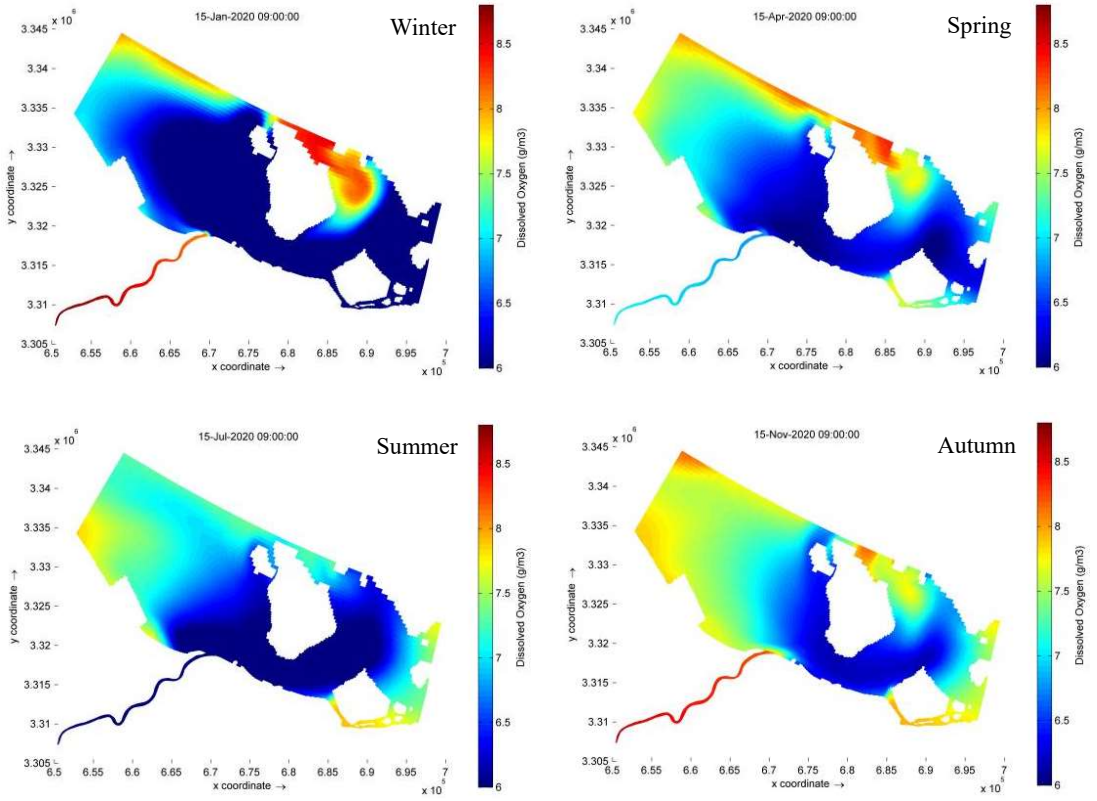

Figure 21. Changes in Dissolved oxygen concentration distribution in the study area during different seasons.

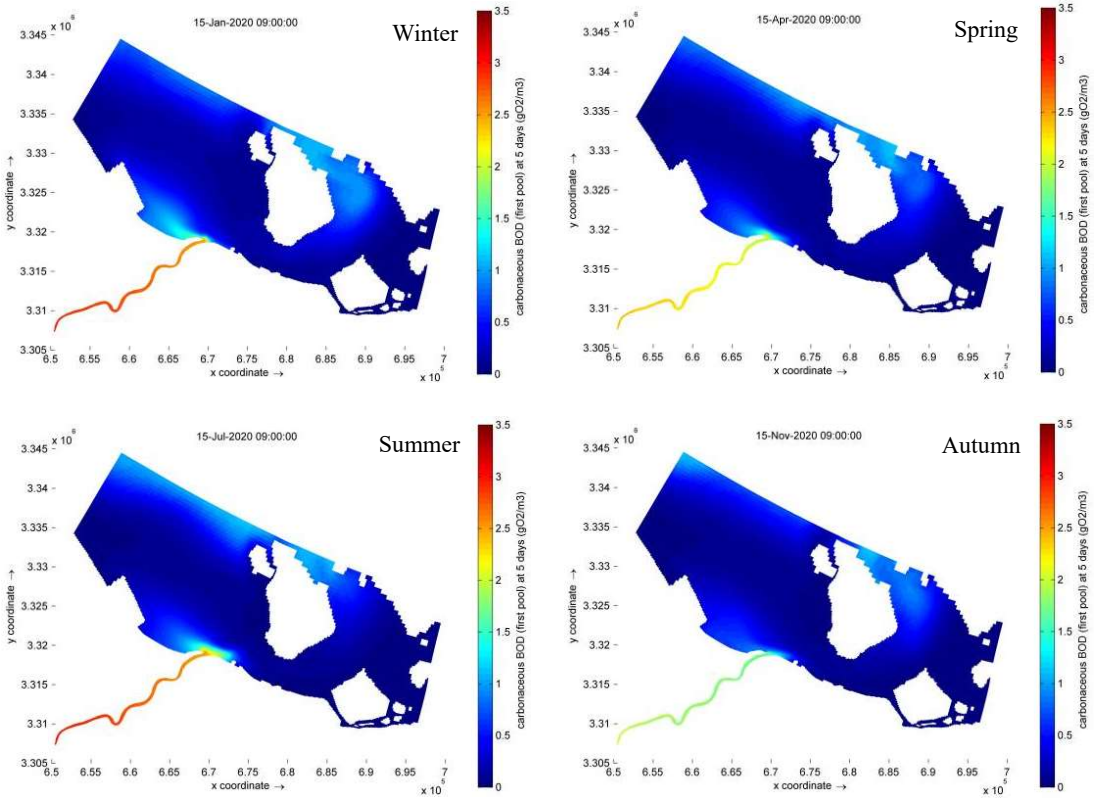

Figure 22. Changes in Biochemical oxygen demand distribution in the study area during different seasons.

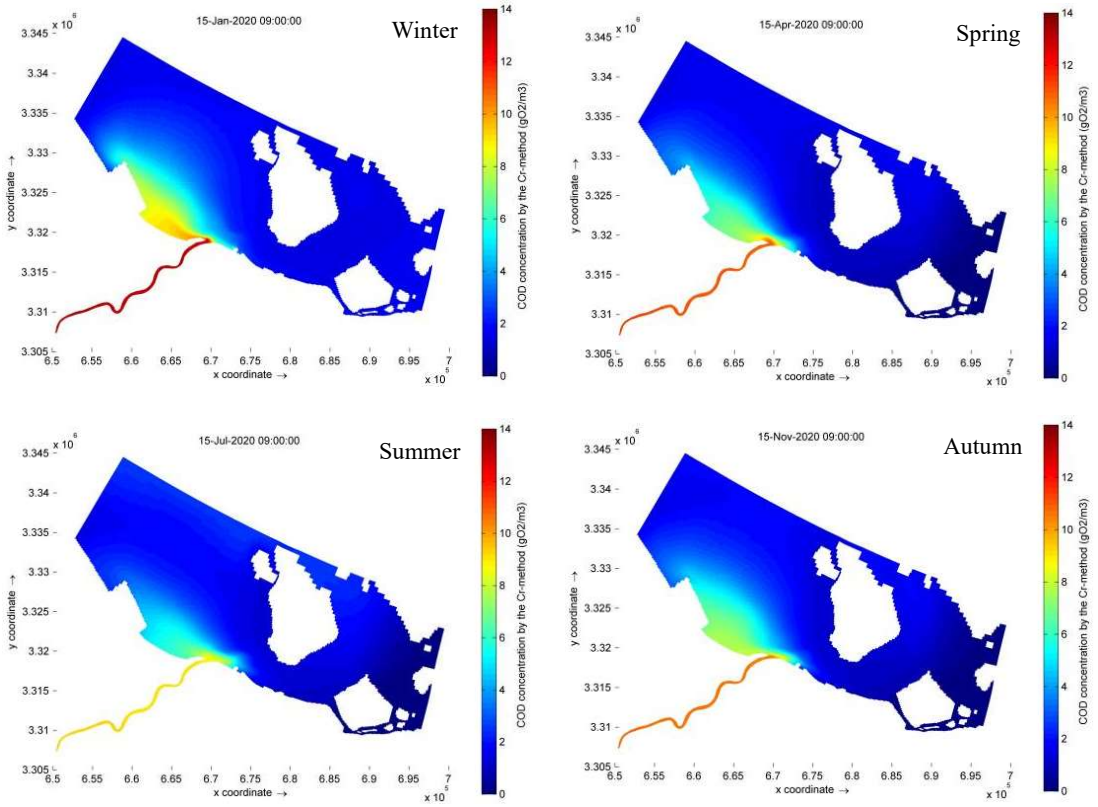

Figure 23. Changes in Chemical oxygen demand distribution in the study area during different seasons.

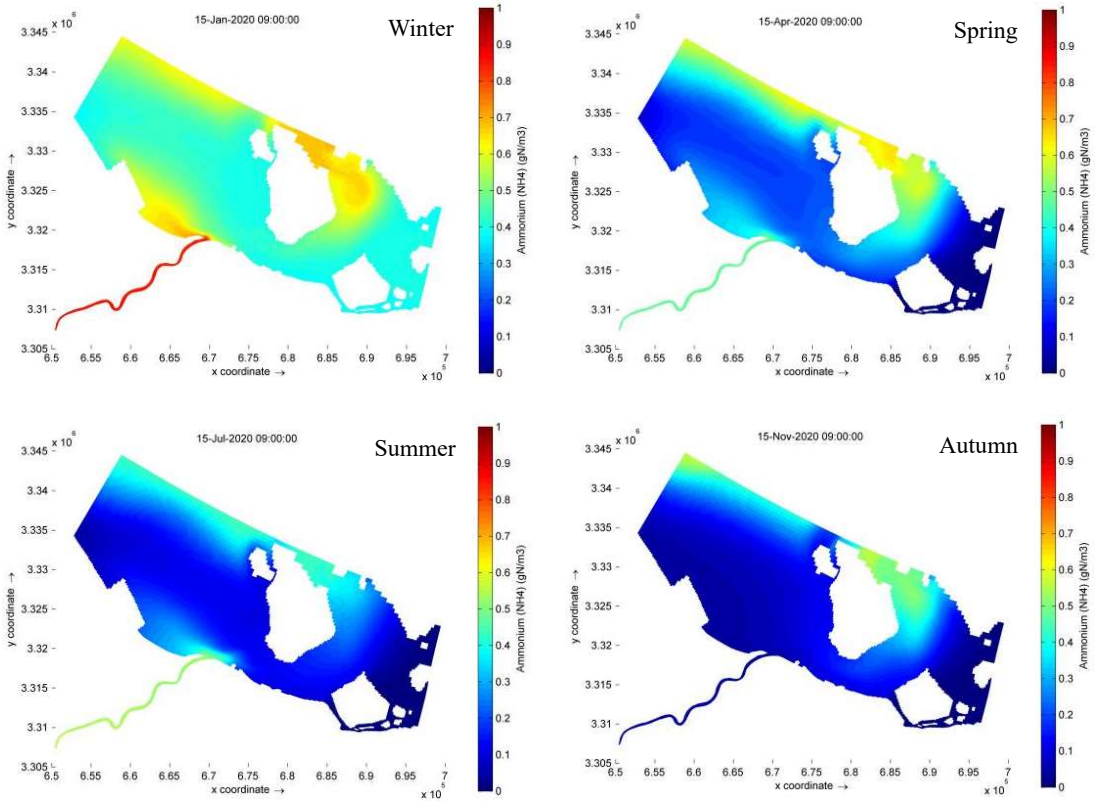

Figure 24. Changes in Ammonium concentration distribution in the study area during different seasons.

5.3 The relationship between hydrodynamic characteristics and water quality

5.3.1 Flow field characteristics

The depth-averaged flow field of the Yong River and offshore waters for the full tidal cycle from July 1st to 2nd is depicted in Figures 25-27. On July 1st, the ebb tide starts at 10:30 p.m. (Figure 25 (a) (b)). At 2.30 a.m. on July 2nd, the ebb tide was still in effect, and the flow velocity in the estuary and offshore area generally dropped (Figure 25 (c) (d)). At 5.00 a.m. on the July 2nd (Figure 25 (e) (f)), the first high tide began. Seawater began to flow from the outer sea to the nearshore and estuary areas, with the estuary flowing at a faster rate than the outer sea. By 7.00 a.m., the high tide was still going strong, and the estuary flow rate had increased (Figure 26 (a) (b)). At 10.30 a.m. the tide will be full and then a new ebb will start (Figure 26 (c) (d)) at 3.30 p.m. on the 2nd the ebb tide trend gradually faded away and a second high tide will start (Figure 25 (e) (f)). By 7.00 p.m. the trend will be similar to that of 7.00 a.m., the flow in the estuary will be higher and the tide in the Jing Tang channel will be in the ebb direction. At this point tide will not have changed, but the flow will have reduced significantly, and the trend will be back to a high tide (Figure 27 (a) (b)). The second high tide reaches full tide at around 10.30 p.m. on the night of the 2nd July (Figure 27 (c) (d)) and then the next day's ebb tide begins, so that the cycle continues.

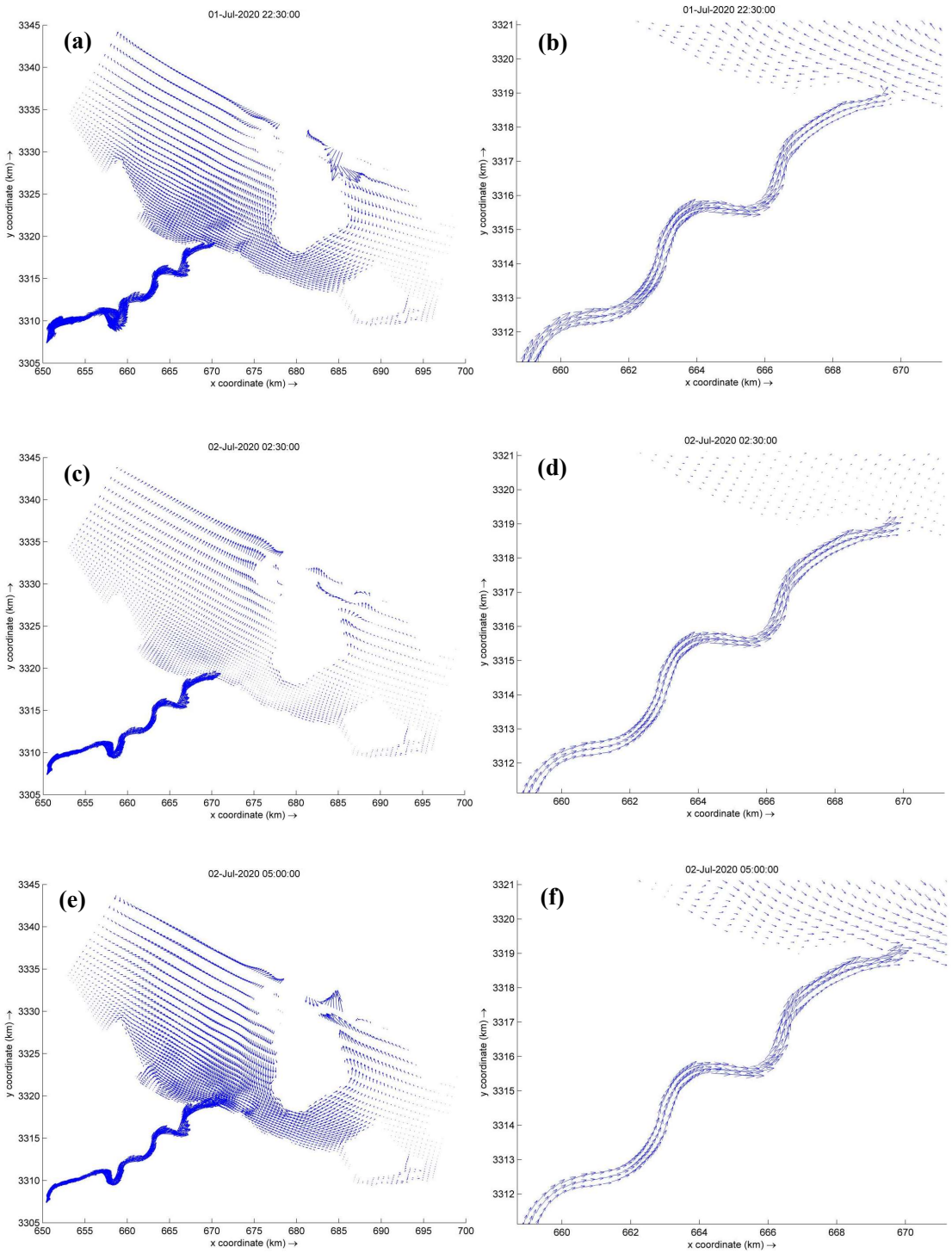

Figure 25. Distribution of the hydrodynamic flow field of the first ebb tide in a full tidal cycle on 1st July, 2020 22:30:00, 2nd July, 2020 02:30:00, and 2nd July, 2020 05:00:00. The arrow indicates depth averaged velocity. (a), (c), and (e) show the sea area near the estuary. (b), (d), and (f) show the part of the Yong River and the estuary.

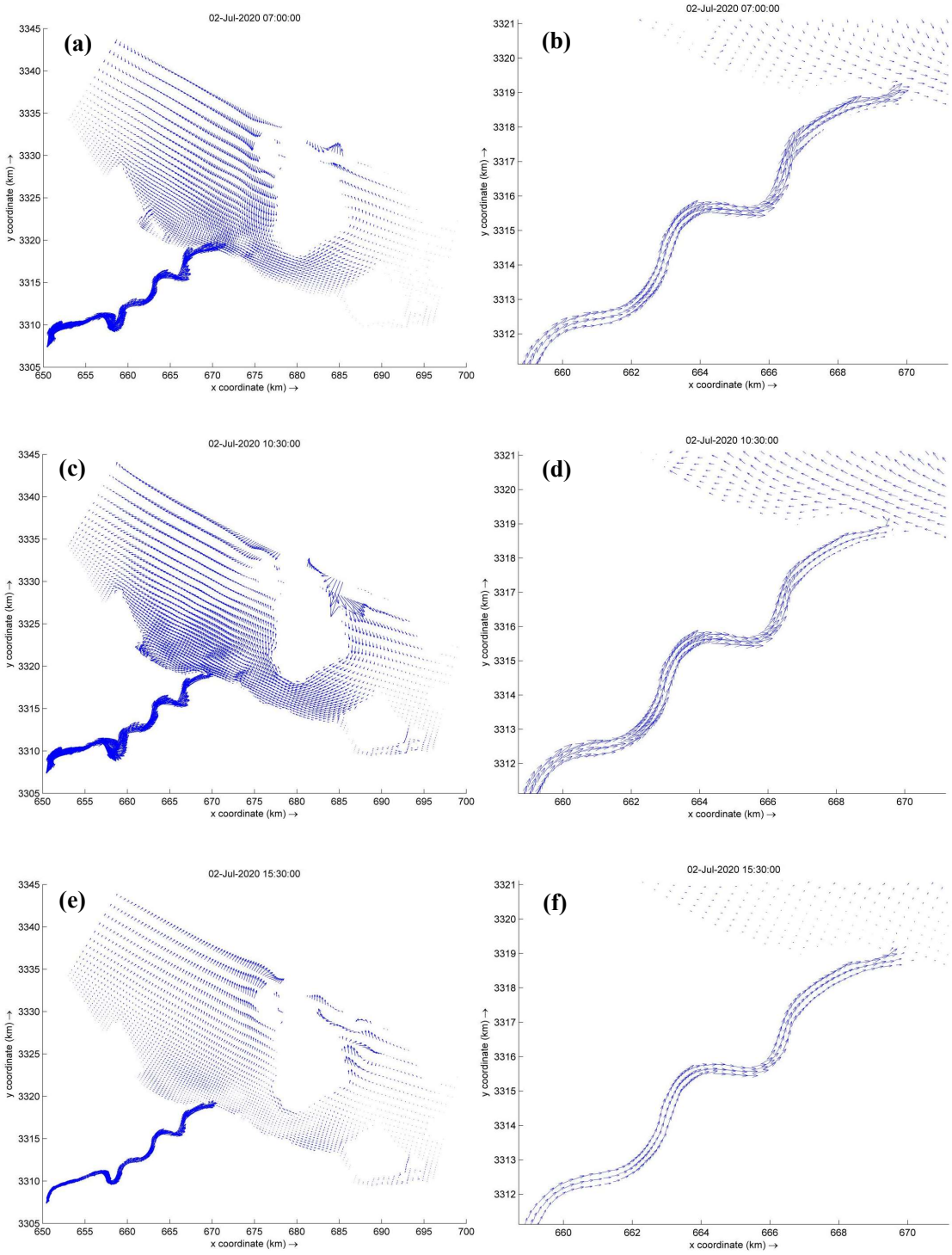

Figure 26. Distribution of the hydrodynamic flow field of the first high tide in a full tidal cycle on 2nd July, 2020 07:00:00, 2nd July, 2020 10:30:00, and 2nd July, 2020 15:30:00. The arrow indicates depth averaged velocity. (a), (c), and (e) show the sea area near the estuary. (b), (d), and (f) show the part of the Yong River and the estuary.

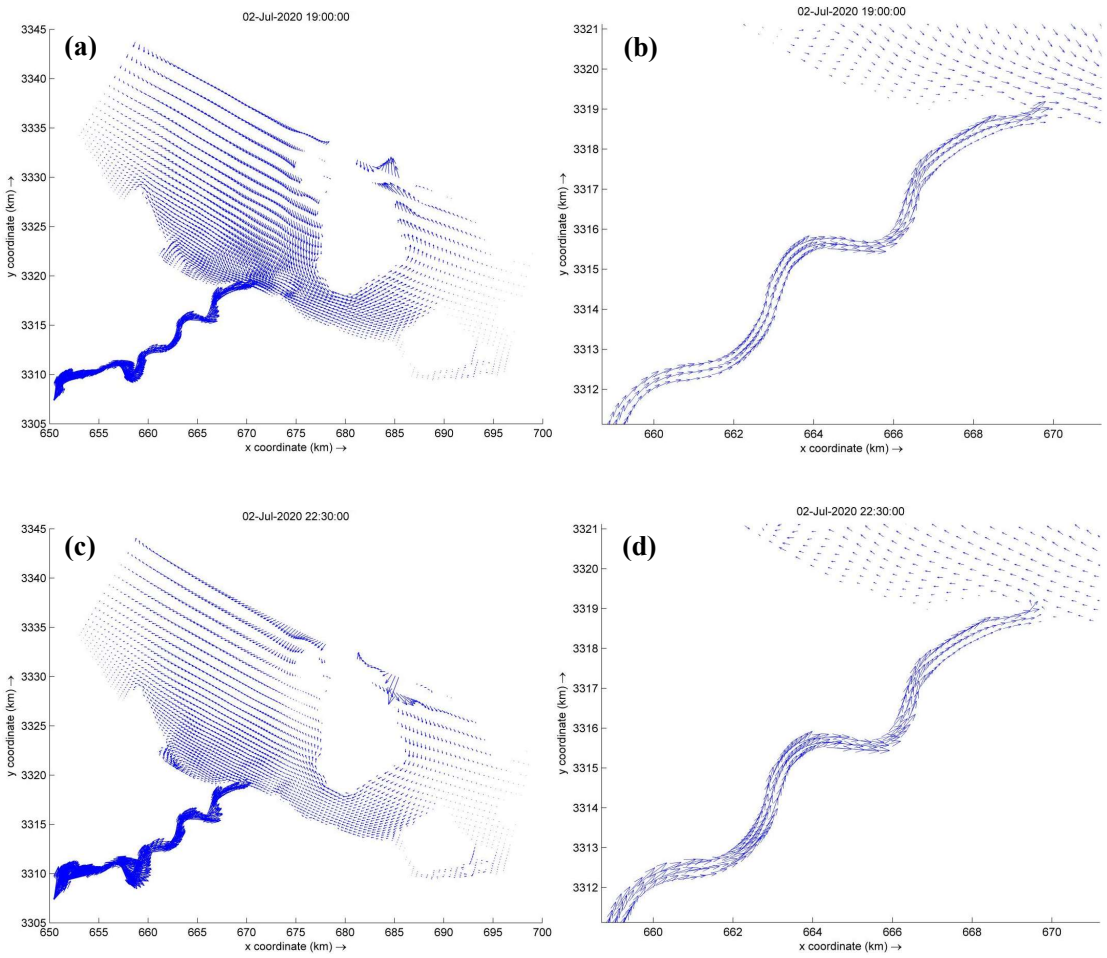

Figure 27. Distribution of the hydrodynamic flow field of the second high tide in a full tidal cycle on 2nd July, 2020 19:00:00 and 2nd July, 2020 22:30:00. The arrow indicates depth averaged velocity. (a) and (c) show the sea area near the estuary, (b) and (d) show the part of the Yong River and the estuary.

The simulation results showed that the tides in the Yong River estuary were indeed irregular semi-diurnal tides, characterized by two high tides and two low tides in one solar day, with intra-day inequalities in tide height and tide time. The outer tidal waves travel in a south-easterly to north-westerly direction towards the inshore waters of Ningbo Zhoushan. The tidal waves pass through various waterways in the internal waters of the Ningbo Zhoushan Islands (around Beilun, Zhenhai), and in the internal Jintang and Luotou waterways of the Ningbo Zhoushan Islands, the high and low tides form a clear reciprocal flow, and the structure of the high and low flow fields is basically the same. Some of the tidal waves that cross the internal waters of the Ningbo Zhoushan Islands and reach the mouth of the Yong River continue to flow upstream along the Yong River channel. In addition, in the waterway near Jintang Island, the tide may be influenced by the topography of the archipelago and the tidal waves from the south-east, and the high tide and low tide are slightly later than in the waters near the estuary. The results are consistent with the actual situation, and the simulation results of the tidal level are sufficient to show that the model has been able to reflect the water

level changes of the Yong River and the sea around the estuary better, providing a better hydrodynamic simulation result for the water quality model.

5.3.2 Impact of estuarine flow characteristics on water quality

Based on the results of 5.3.1, we confirmed the results of the hydrodynamic model and then combined the characteristics of the NH_4^+ dilution and diffusion concentration field with the corresponding flow field diagrams to investigate the relationship between hydrodynamic and water quality in the estuary.

The NH_4^+ concentration distribution in a full tidal cycle is analysed by combining the characteristics of the NH_4^+ dilution diffusion concentration field with the corresponding flow field diagram. After entering the sea from the estuary, the water of the Yong River dilutes and diffuses upstream or downstream with the rising and falling tides under the effect of turbulent and convective diffusion caused by the complex estuarine current conditions, and the degree of diffusion varies with the hydrological conditions. From a full tidal cycle from 1st to 2nd July (Figures 28-29), Figure 28 (a) (b) shows the ebb tide phase, when the flow direction of the Yong River estuary was all directed to the west side of the estuary, and Ammonium salt reaching the estuary began to spread along the coast to the west side of the estuary. Ebb tide continued at 2.30 a.m. on 2nd July, and the total flow velocity in the estuary and offshore area decreased, and Ammonium salt had already distributed to the total flow rate in the estuary and offshore area decreased at 2.30 a.m. on 2nd July, with Ammonium salt already distributed to the west side of the estuary (Figure 28 (c) (d)). The first high tide starts at 5.00 a.m. when the seawater moves from the outer inshore and estuarine areas, the direction of the estuarine current changes to the east side of the estuary and the current carries Ammonium salt also to the east side of the estuary. The high tide will be full at 10.30 a.m. (Figure 28 (e) (f)), followed by a new ebb tide. At 3.30 p.m. the ebb trend will gradually subside, the flow to the west of the estuary will decrease and the current will again carry Ammonium salt to the east of the estuary (Figure 29 (a) (b)). The trend at 7.00 p.m. will be similar to 7.00 a.m., the flow in the estuary will be high and the tide in the direction of the tide, which will not change at this point, but the flow will be significantly reduced, and Ammonium salt will accumulate in the estuary with a significant increase in concentration (Figure 29 (c) (d)). The second high tide reaches full tide at around 10.30 p.m. the following day (Figure 29 (e) (f)), after which the direction of flow in the estuary reverses again and the current carrying Ammonium salt begins to transport to the west of the estuary.

The comparison in the Figures 36-41 show that the advection of pollutants in the estuary follows the rise and fall of the tide, and the direction of advection is significantly influenced by the direction of the water flow at high and low tides. At high tide, seawater intrusion intensifies, and pollutants follow the upward flow of the rising tide. At low tide, the tide may be influenced by the topography of the archipelago and the south-eastern tidal waves in the channel near Jintang Island, with high and low tide

slightly later than the waters near the estuary, making the diffusion of pollutants to the east side of the estuary at low tide less pronounced than to the west side of the estuary at high tide. Therefore, in a full tidal cycle of falling rapid, falling rest, rising rapid and rising stop, the influence of islands on the east side of the Yong River estuary at low tide and the complex topography of many channels make the eastern part of the area inconsistent with the western side at high and low tide times, which is most unfavourable to the diffusion of pollutants.

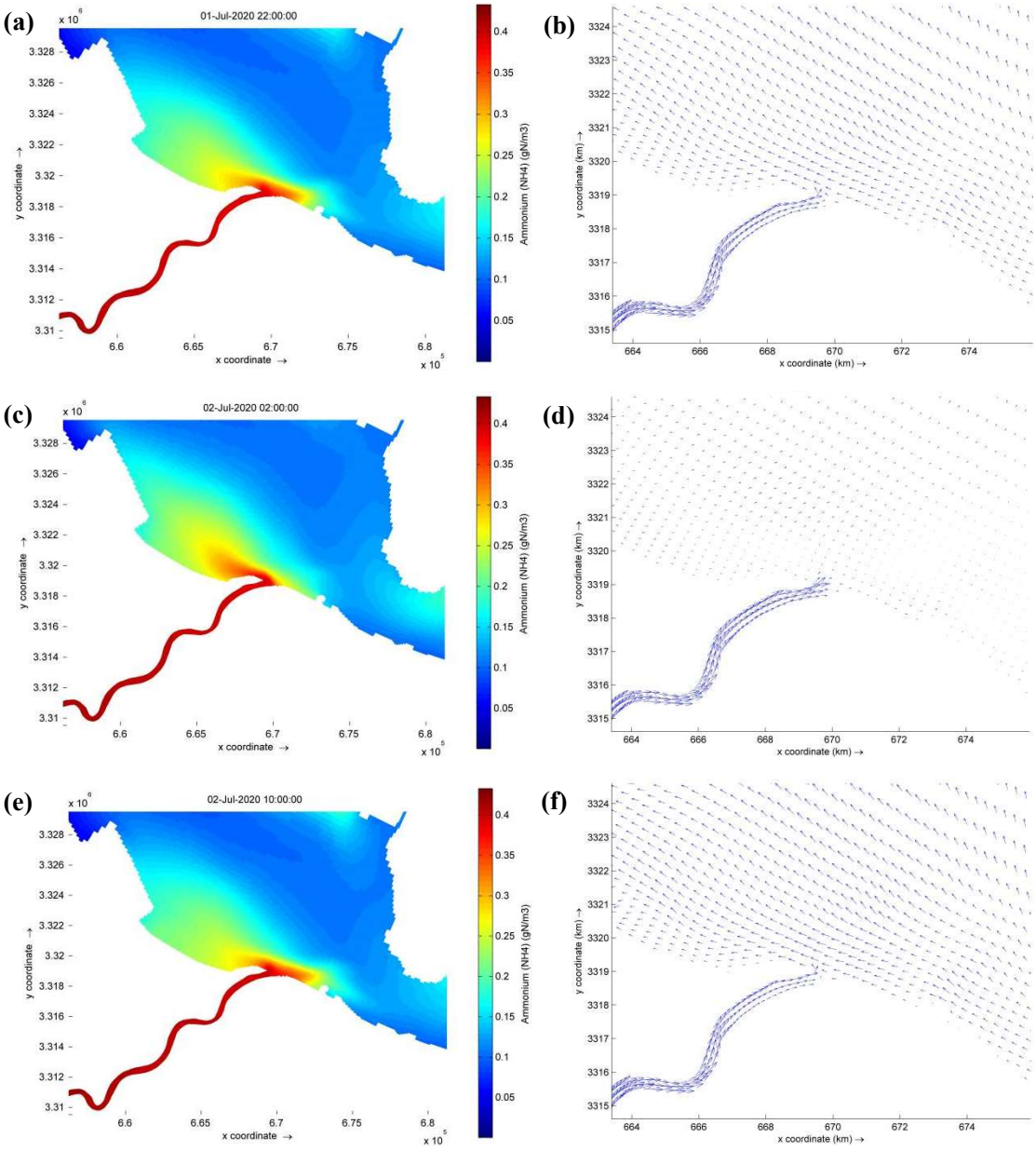

Figure 28. The distribution of NH_4^+ concentration and the estuary flow field on 1st July, 2020 22:00:00, 2nd July, 2020 19:00:00, and 2nd July, 2020 10:00:00. (a), (c), and (e) show the NH_4^+ concentration distribution. (b), (d), and (f) show the characteristics of the flow field.

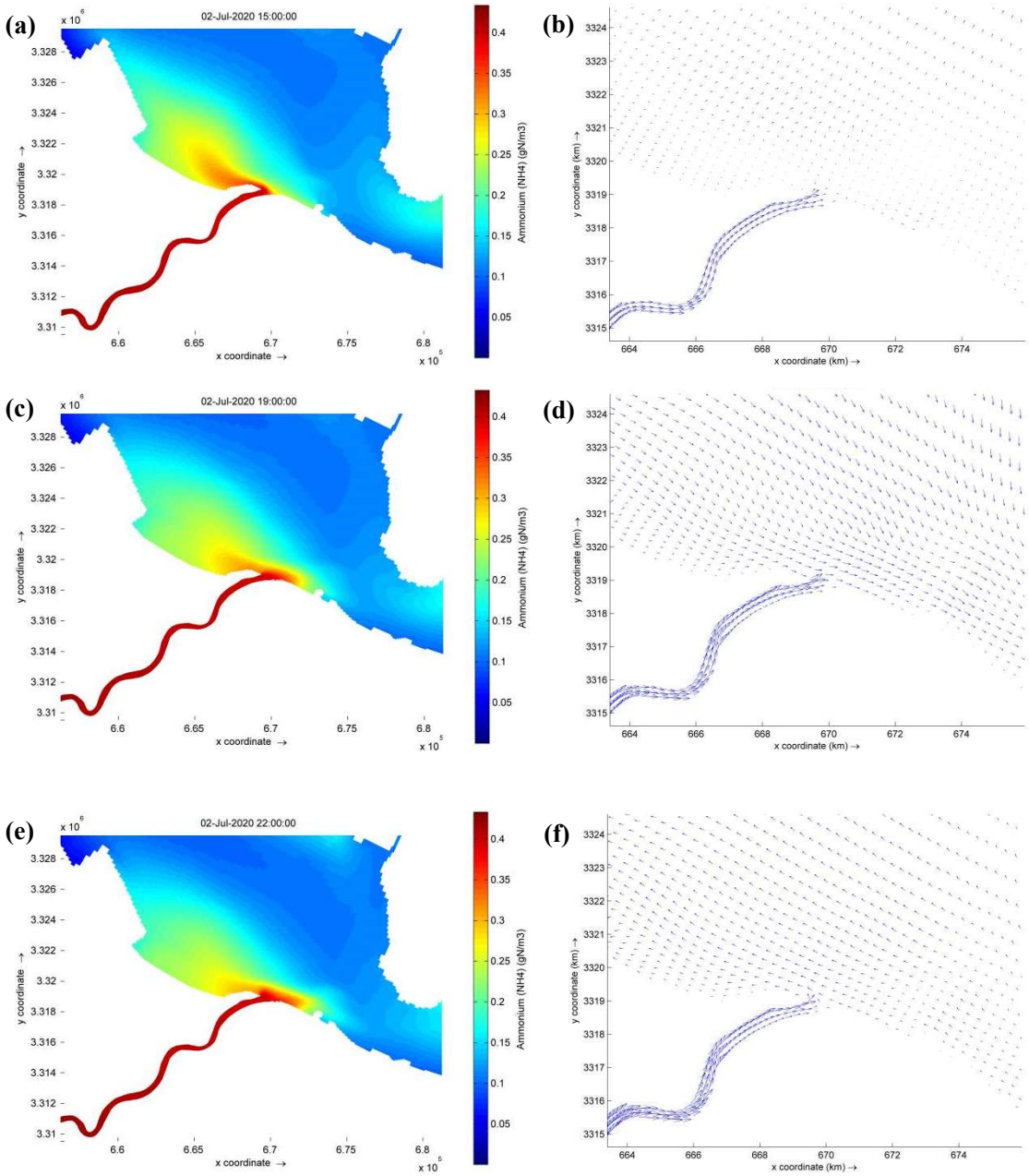

Figure 29. The distribution of NH_4^+ concentration and the estuary flow field on 2nd July, 2020 15:00:00, 2nd July, 2020 02:00:00, and 2nd July, 2020 22:00:00. (a), (c), and (e) show the NH_4^+ concentration distribution. (b), (d), and (f) show the characteristics of the flow field.

6. Discussion

6.1 Estuarine hydrodynamics and water quality characteristics

The mainstream of the Yong River was originally a natural tide-sensitive section with good water depth and a relatively stable riverbed. Since the 1950s, the Yao River channel and the mainstream of the Yong River have been used for tidal storage and economic development. With the construction of the Yao River Gate, the Zhenhai Port area, the Sea Barrier, the Out-of-Mouth Diversion Dike and the T-share Dam respectively, causing changes in the tidal wave propagation and sediment movement patterns of the Yong River, reducing the tidal capacity and causing serious siltation of the riverbed. In recent years, a large number of water-related projects have been built in the Yong River basin, which, while promoting the economic development of the basin, have also changed the material transport and energy fluxes in the middle and lower reaches (Zhang et al., 2018). The Yong River estuary is a typical curved transitional estuary, where the tidal wave propagation characteristics of the river depend on the local topography, upstream runoff, and tidal waves outside the mouth. The flow direction and velocity of the Yong River estuary are influenced by irregular semi-diurnal tides, and the concentration distribution of water quality parameters in the estuary varies with the tidal conditions.

Findings here support the concept that the hydrodynamic cyclicity of the coastal river and ocean tides has a more pronounced effect on water quality. For instance, in the study of Lake Nokoué (Benin, West Africa), Djihouessi and Aina (2018) found that, when compared to dissolved oxygen levels in other parts of the lake, the diurnal oxygen cycle in Lake Nokoué shows notable variances, due to the geomorphology of the coastal river inflow and open to the Atlantic Ocean, which resembles a semi-enclosed estuary. In the early morning this oxygen content gradually increases during the day and the sharp drop in dissolved oxygen concentration at night. During high water levels, the mean salinity of the lake is kept at an extremely low level by freshwater intake from the Norquay streams. During low water levels, the intrusion of seawater into Lake Norquay is higher than the freshwater input, leaving the whole lake still brackish with an average salinity of about 15 ppt. Meanwhile, Iqbal et al. (2019) also used Water Quality Analysis Simulation Program (WASP 8.1) and LOADEST to assesses the water quality and nutrient load discharged into the West Sea of the coastal river waterfront (Tamjin River). Significant seasonal differences in pollution loads in the coastal waterfront were also found to influence the development of red tides.

In addition, Lilian Seiler et al. (2020) through the application of three-dimensional numerical modelling to understand the complex estuarine system the Santos-São Vicente-Bertioga estuarine system (Brazil). The system's overall circulation demonstrates that the system's sub-environments are essential to its functioning, with strong flows and less dynamic areas in the main channels concentrated within the estuary and near the large intertidal zone. The water flow between the estuary and

nearby coastal waters is regulated by this pattern. The findings demonstrate that within a single estuary channel, subregions with various hydrodynamic behaviours are produced by the interaction of river discharge and channel shape. This is also consistent with our finding that the tides near the Jintang channel do not coincide with the timing of high and low tides on the western side of the estuary due to topographic influences.

The hydrodynamic circulation in the estuary also influences the transport of pollutants. Matilda Mali carried out a two-dimensional numerical simulation using MIKE21 software to determine the sources and fate of pollutants within the Torre a Mare port (Italy). A comparative analysis of the modelled response with the actual metal contaminant distribution shows a high degree of agreement, indicating that the contaminants mainly originate come from outside the port and tend to accumulate inside the basin. Indeed, the hydrodynamic circulation leads to river flow into the harbour entrance, while the specific harbour morphology makes it difficult for fine sediments to be exported from the inner basin, thus increases the concentration of sediment-associated contaminants within the harbour area. The study supports that the quality of the tourist harbour area is heavily dependent on the sources of pollution within and outside the harbour area and is largely controlled by hydrodynamically driven processes (Mali et al., 2018). Michele Arienzo et al. (2022) also summarizes the factors affecting the transport of Rare Earth Elements, REE, in coastal estuaries. In organic-rich rivers, the transport of REEs in the water column can be 100% dependent on the colloidal material in the water. In estuaries, however, because of the characteristics of the estuary, the mixing process of fresh and salt water can lead to the sedimentation of colloidal and particle-bound lanthanides after they have solidified, with removal rates ranging from 30% to 90%. In this case, the reduction of rare earth elements in rivers may then not be a reduction from river to brackish water to seawater, but there will be a significant reduction in concentration in the estuary.

6.2 Influencing factors of coastal rivers and estuarine water environments

The study area's water level simulation findings show that the difference between the simulated and measured water levels at the river's monitoring locations is rather noticeable. From the entrance upstream to the sea around the estuary, there is an increasing trend in the degree of match between the simulated and measured water levels. The difference between modelled and actual values is less at monitoring locations near the estuary than along the river. With a better fit of the simulated results at certain spots along the river, the similar tendency is seen for water quality. The measured values at the two seawater quality monitoring stations close to the estuary and the coast were more closely matched by the simulated values. However, the modelled values for each parameter deviate further from reality the farther out at sea. This might be connected to the river's use of gates to artificially control the amount of water flowing into the mainstream. By observing the Suwol-dong River's flow and water quality while the gates were open at Daejeon and Hwangsan, Hwang (2014)discovered that the water quality of the river declined when the gates were

opened by 3% to 38% according to the typical steady-state model QUAL2E and the unsteady-state model CE-QUAL-RIV1. The opening of the gates causes a 3% – 38% drop in water quality.

Additionally, the Yong River estuary is also a significant port surrounded by several channels and regular ships. It is anticipated that the numerous ships and frequent shipping may also have an impact on the Yong River estuary's water quality. In this study, we did not include shipping activities to the modelling processes due to data availability. However, a related study was carried out by Sharma et al. (2021), who used hydrodynamic modelling in the Kolkata Port Trust (Kolkata, West Bengal, India) to investigate the relationship between sediment advection and shipping channels. Results obtained from the Kolkata Port Trust's hydrodynamic modelling simulations indicate that the sediment advection pattern, which is influenced by the channel, initially running parallels the regular shipping channels and then moves away from it. Investigations at the Lower Auckland Mine site with a lower degree of sediment advection also indicated that the sediment tended to move along the shipping channels. The study suggests that there is a correlation between the trajectory of estuarine material movement and the location of the channel, and that shipping activities also have an impact on the estuarine water environment.

7. Conclusion

This thesis summarizes the research background and significance of numerical simulation of water quality in the inlet rivers and offshore areas and compares the research progress of hydrodynamic water quality models. Facing the water environment problems of the Yong River and its estuary, a three-dimensional coupled hydrodynamic water quality model is established based on Delft3D software, and the simulation results of the model are compared and verified and analysed. Based on the work of this study, the main conclusions can be drawn as following：

(a) The three-dimensional hydrodynamic model of the Yong River and the offshore area of the estuary established in this paper takes into account the role of the tidal field and provides a reasonable verification of the water level and tide in the sea near the Yong River and the estuary, which can provide stable flow field conditions for the water quality model. From the simulation results, the Yong River and the sea area near the estuary are dominated by tidal currents in the past complex flow pattern, with the flow velocity at low tide greater than that at high tide, and the flow velocity in the river channel greater than that in the estuary.
(b) The water quality model established in this paper considers five main water quality variables (DO, COD, BOD5, NH_4^+, PO_4^{3-}) and involves four main reaction processes, determines the main parameters of water quality through parameter rate determination, and conducts error analysis on the simulation results, the simulation results are basically consistent with the measured values, providing a basis for further research on the distribution of water quality parameter concentrations in the estuary area.
(c) The hydrodynamic periodicity of the coastal river and ocean tides has a more pronounced effect on the concentration distribution of water quality parameters. The position of the concentration distribution of water quality measures in the estuary area is affected by the tide. At low tide, pollutants generally spread to the west side of the estuary, while at high tide, the eastern side of the Yong River estuary is not consistent with the western side at high and low tide due to the complex topography of the eastern side of the estuary and the influence of islands and navigation channels, which is not conducive to the advection of pollutants.

The three-dimensional hydrodynamic and water quality model developed in this thesis can reflect the hydrodynamic and water quality conditions of the Yong River and the sea near the estuary to a certain extent, which is useful for decision-making on the water environment in the near-shore area, and also has some reference significance for the hydrodynamic and water quality modelling in other areas.

References

Afshar, A., Kazemi, H., & Saadatpour, M. (2011). Particle Swarm Optimization for Automatic Calibration of Large Scale Water Quality Model (CE-QUAL-W2): Application to Karkheh Reservoir, Iran. Water Resources Management, 25(10), 2613–2632. https://doi.org/10.1007/s11269-011-9829-7

Ahn, J., Na, Y., & Park, S. W. (2019). Development of Two-Dimensional Inundation Modelling Process using MIKE21 Model. KSCE Journal of Civil Engineering, 23(9), 3968–3977. https://doi.org/10.1007/s12205-019-1586-9

Akkoyunlu, A., & Karaaslan, Y. (2015). Assessment of improvement scenario for water quality in Mogan Lake by using the AQUATOX Model. Environmental Science and Pollution Research, 22(18), 14349–14357. https://doi.org/10.1007/s11356-015-5027-0

Alipoor, V., Rahimibashar, M. R., & Aliev, A. (2011). Temporal and spatial variation of macrozoobenthos in the Chamkhale Estuary (South Caspian Sea). Middle-East Journal of Scientific Research, 10(5), 654-658.

Al-Murib, M. (2014). Application of CE-QUAL-W2 on Tigris River in Iraq. Civil and Environmental Engineering Master's Project Reports. https://doi.org/10.15760/CEEMP.26

Arienzo, M., Ferrara, L., Trifuoggi, M., & Toscanesi, M. (2022). Advances in the Fate of Rare Earth Elements, REE, in Transitional Environments: Coasts and Estuaries. Water, 14(3), 401. https://doi.org/10.3390/w14030401

Benitez-Nelson, C. R. (2000). The biogeochemical cycling of phosphorus in marine systems. Earth-Science Reviews, 51(1-4), 109-135. https://doi.org/10.1016/S0012-8252(00)00018-0

Blumberg, A. F., & Mellor, G. L. (1987). A Description of a Three-Dimensional Coastal Ocean Circulation Model. Three-Dimensional Coastal Ocean Models, pp. 1-16. American Geophysical Union (AGU). https://doi.org/10.1029/CO004p0001

Bricker, S. B., Rice, K. C., & Bricker, O. P. (2014). From Headwaters to Coast: Influence of Human Activities on Water Quality of the Potomac River Estuary. Aquatic Geochemistry, 20(2-3), 291-323. https://doi.org/10.1007/s10498-014-9226-y

Cashel, F., & Knightes, C. (2021). Mechanistic Modeling Using the Water Quality Analysis Simulation Program (WASP8): Assessing Eutrophication in the Pawcatuck River Estuary. 2021, B35F-1482.

Chen J., & Chen S. (2002). Challenges for China's estuarine coast. Marine Geology Letters (01), 1-5, 3. (In Chinese)

Chen, C., Huang, H., Beardsley, R. C., Xu, Q., Limeburner, R., Cowles, G. W., Sun, Y., Qi, J., & Lin, H. (2011). Tidal dynamics in the Gulf of Maine and New England Shelf: An application of FVCOM. Journal of Geophysical Research: Oceans, 116(C12). https://doi.org/10.1029/2011JC007054

Chin, D. A. (2012). Water-quality engineering in natural systems: fate and transport processes in the

water environment. John Wiley & Sons.

Cole, T., & Wells, S. (2006). CE-QUAL-W2: A Two-dimensional, Laterally Averaged, Hydrodynamic and Water Quality Model, Version 3.5. Civil and Environmental Engineering Faculty Publications and Presentations. https://pdxscholar.library.pdx.edu/cengin_fac/130

Davies, A. M., Jones, J. E., & Xing, J. (1997). Review of Recent Developments in Tidal Hydrodynamic Modeling. I: Spectral Models. Journal of Hydraulic Engineering, 123(4), 278–292. https://doi.org/10.1061/(ASCE)0733-9429(1997)123:4(278)

Deltares, D. (2017). Delft3d-flow user manual. Deltares Delft, The Netherlands, 686.

Deltares, D. (2020). Delft3d-water quality user manual. Deltares Delft, The Netherlands, 382.

Department of Ecology and Environment of Zhejiang Province. (2021). 2021 Zhejiang Province Ecological Environment Status Bulletin, 33. (In Chinese)

Djihouessi, M. B., & Aina, M. P. (2018). A review of hydrodynamics and water quality of Lake Nokoué: Current state of knowledge and prospects for further research. Regional Studies in Marine Science, 18, 57-67. https://doi.org/10.1016/j.rsma.2018.01.002

Dobbins, W. E. (1964). Bod and oxygen relationship in streams. Journal of the Sanitary Engineering Division, 90. https://doi.org/10.1061/JSEDAI.0000495

Egbert, G. D., & Erofeeva, S. Y. (2002). Efficient inverse modeling of barotropic ocean tides. Journal of Atmospheric and Oceanic technology, 19(2), 183-204. https://doi.org/10.1175/1520-0426(2002)019<0183:EIMOBO>2.0.CO;2

Elias, E., Walstra, D.-J., Roelvink, D. J. A., Stive, M., & Klein, M. (2001). Hydrodynamic Validation of Delft3D with Field Measurements at Egmond (p. 2727). https://doi.org/10.1061/40549(276)212

Festa, J. F., & Hansen, D. V. (1976). A two-dimensional numerical model of estuarine circulation: The effects of altering depth and river discharge. Estuarine and Coastal Marine Science, 4(3), 309–323. https://doi.org/10.1016/0302-3524(76)90063-3

Gross, P., & Railton, E. P. (1972). Teaching science in an outdoor environment. University of California Press.

Howland, W. E., & Thomas, H. A. J. (1949). Pollution load capacity of streams. Water & Sewage Works, 96(7), 264-266.

Hu J., & Lee Y. (2008). One-dimensional salinity and three-dimensional baroclinic coupled model for simulating the flow in Pearl River delta. Journal of Hydraulic Engineering, (11), 1174-1182.

Huang W. (2013). Contents and sources of organic colloid and its effect on heavy metals behavior in Yangtze River Estuary. East China Normal University. (In Chinese)

Huybrechts, N., Villaret, C., & Lyard, F. (2012). Optimized Predictive Two-Dimensional Hydrodynamic Model of the Gironde Estuary in France. Journal of Waterway, Port, Coastal, and Ocean Engineering, 138(4), 312–322. https://doi.org/10.1061/(ASCE)WW.1943-5460.0000129

Hwang, J. Y., Kim, Y. D., Kwon, J. H., Park, J. H., Noh, J. W., & Yi, Y. K. (2014). Hydrodynamic

and water quality modeling for gate operation: A case study for the Seonakdong River basin in Korea. KSCE Journal of Civil Engineering, 18(1), 73-80. https://doi.org/10.1007/s12205-013-0025-6

Iqbal, M. M., Shoaib, M., & Agwanda, P. O. (2019). The response of pollution load from coastal river waterfront on red tides in South Sea. Journal of Coastal Research, 91(SI), 231-235.

Ji, Z. G. (2017). Hydrodynamics and water quality: modeling rivers, lakes, and estuaries. John Wiley & Sons.

Jiang Y., Zhu F., & Geng S. (2011). Exploring the problem of offshore marine dumping in Zhoushan City. Journal of China Foreign Investment, (16), 176, 178.

Kepesidi, A., Pavlou, P., Vroom, I., & Zamparutti, T. (2022). The United Nations Ocean Conference, 27 June-1 July 2022, Lisbon, Portugal.

Kim, C. K., Park, K., Powers, S. P., Graham, W. M., & Bayha, K. M. (2010). Oyster larval transport in coastal Alabama: Dominance of physical transport over biological behavior in a shallow estuary. Journal of Geophysical Research: Oceans, 115(C10). https://doi.org/10.1029/2010JC006115

Kim, J., Lee, T., & Seo, D. (2017). Algal bloom prediction of the lower Han River, Korea using the EFDC hydrodynamic and water quality model. Ecological Modelling, 366, 27–36. https://doi.org/10.1016/j.ecolmodel.2017.10.015

Kuang C., Lee X., & Liu S. (2009). Effect of Large Scale Reclamation on Hydrodynamic Circulation in Victoria Harbour of Hong Kong. Journal of Tongji University (Natural Science), (02), 176-181, 252. (In Chinese)

Lai Z. (2002). Study on 1-D & 3-D hydrodynamic and water quality models coupling computation of the Pearl River Delta network and sea area. Sun Yat-sen University. (In Chinese)

Lai, Z., Chen, C., Cowles, G. W., & Beardsley, R. C. (2010). A nonhydrostatic version of FVCOM: 1. Validation experiments. Journal of Geophysical Research: Oceans, 115(C11). https://doi.org/10.1029/2009JC005525

Lakshmi, A., & Rajagopalan, R. (2000). Socio-economic implications of coastal zone degradation and their mitigation: A case study from coastal villages in India. Ocean & Coastal Management, 43(8–9), 749–762. https://doi.org/10.1016/S0964-5691(00)00057-0

Leendertse, J. J., & Liu, S. K. (1975). Modeling of Three-Dimensional Flows in Estuaries. ASCE.

Lesser, G. R., Van Kester, J., Walstra, D. J. R., & Roelvink, J. A. (2001). Three-dimensional morphological modelling in Delft3D-FLOW.

Liu J.， Liu L.， & Zhang B. (2017). Problems and countermeasures of water environmental management in estuaries. Research of Environmental Sciences, 30(5) , 645-653． (In Chinese)

Liverman, D., Rockström, J., Visbek, M., Leemans, R., Abrahamse, T., Becker, B., ... & Seitzinger, S. P. (2013). Future earth initial design (No. 1). ICSU.

Long J., & Lee Y. (2007). Finite element method combining the 1-D & 3-D hydrodynamic modeling

of the Pearl River outlets. Journal of Hydrodynamics, A(04), 512-519. (In Chinese)

Luo Y. (2016). Sustainability Associated Coastal Eco-environmental Problems and Coastal Science Development in China. Bulletin of Chinese Academy of Sciences, 31(10), 1133-1142. (In Chinese)

Mali, M., Malcangio, D., Dell'Anna, M. M., Damiani, L., & Mastrorilli, P. (2018). Influence of hydrodynamic features in the transport and fate of hazard contaminants within touristic ports. Case study: Torre a Mare (Italy). Heliyon, 4(1), e00494. https://doi.org/10.1016/j.heliyon.2017.e00494

Martin, J., McCutcheon, S., & Schottman, R. (1999). Hydrodynamics and transport for water quality modeling. Boca Raton: Lewis. https://doi.org/10.1201/9780203751510

Martin, J.L., Ainbrose, R. & Mccutcheon, S. (1990). Technical Guidance Manual for Performing Waste Load Allocations, Book III: Estuaries. U.S. Environmental Protection Agency Office of Water, Washington, DC.

Martínez, M. L., Intralawan, A., Vázquez, G., Pérez-Maqueo, O., Sutton, P., & Landgrave, R. (2007). The coasts of our world: Ecological, economic and social importance. Ecological Economics, 63(2-3), 254-272. https://doi.org/10.1016/j.ecolecon.2006.10.022

Meire, P., Ysebaert, T., Damme, S. V., Bergh, E. V. D., Maris, T., & Struyf, E. (2005). The Scheldt estuary: a description of a changing ecosystem. Hydrobiologia, 540(1), 1-11.

Milliman, J. D., & Farnsworth, K. L. (2013). River discharge to the coastal ocean: a global synthesis. Cambridge University Press.

Mills, W. B. (1985). Water quality assessment: A screening procedure for toxic and conventional pollutants in surface and ground water. Environmental Research Laboratory, Office of Research and Development, US Environmental Protection Agency.

Ministry of Ecology and Environment, PRC. (2021). 2021 China Marine Ecological Environment Quality Bulletin. (In Chinese)

Neal, C., House, W., Jarvie, H., & Eatherall, A. (1998). The significance of dissolved carbon dioxide in major lowland rivers entering the North Sea. Science of The Total Environment, 210–211, 187–203. https://doi.org/10.1016/S0048-9697(98)00012-6

Needham, S. E., Young, R. A., Ft, S., & Nezdhw, S. E. (1993). ANN-AGNPS: A Continuous Simulation Watershed Model. Proceedings of the Federal Interagency Workshop on Hydrologic Modeling Demands for the 90's. U.S. Geological Survey Water-Resources Investigations Report, 93–4018.

Njiru, M., Nyamweya, C., Gichuki, J., Mugidde, R., Mkumbo, O., & Witte, F. (2012). Increase in anoxia in Lake Victoria and its effects on the fishery. Anoxia, 99-128.

O'Connor, D. J. (1967). The temporal and spatial distribution of dissolved oxygen in streams. Water Resources Research, 3(1), 65–79. https://doi.org/10.1029/WR003i001p00065

Officer, C. B. (1980). Box models revisited. Estuarine and Wetland Processes, pp.65-114. https://doi.org/10.1007/978-1-4757-5177-2_4

Olabarrieta, M., Warner, J. C., & Kumar, N. (2011). Wave-current interaction in Willapa Bay.

Journal of Geophysical Research, 116(C12), C12014. https://doi.org/10.1029/2011JC007387

Park, R. A., Clough, J. S., & Wellman, M. C. (2008). AQUATOX: Modeling environmental fate and ecological effects in aquatic ecosystems. Ecological Modelling, 213(1), 1–15. https://doi.org/10.1016/j.ecolmodel.2008.01.015

Perillo, G. M. (1995). Chapter 2 definitions and geomorphologic classifications of estuaries. Developments in Sedimentology, 53,17-47. https://doi.org/10.1016/S0070-4571(05)80022-6

Pernetta, J. C., & Milliman, J. (1995). Land-Ocean Interactions in the Coastal Zone (LOICZ). Implementation Plan. Global Change Report, (33), 215.

Phelps, E. B., & Streeter, H. W. (1958). A study of the pollution and natural purification of the Ohio River. US Department of Health, Education, & Welfare. http://udspace.udel.edu/handle/19716/1590

Pritchard, A. E. (1960). A new classification of the paedogenic gall midges formerly assigned to the subfamily Heteropezinae (Diptera: Cecidomyiidae). Annals of the Entomological Society of America, 53(3), 305-316. https://doi.org/10.1093/aesa/53.3.305

Pritchard, D. W. (1967). What is an estuary: physical viewpoint. American Association for the Advancement of Science. http://hdl.handle.net/1969.3/24383

Qi J. (2021). Study on the Spatio-Temporal Changes of Eutrophication in Zhejiang Coastal Sea. Zhejiang University.

Qi, J., Chen, C., Beardsley, R. C., Perrie, W., Cowles, G. W., & Lai, Z. (2009). An unstructured-grid finite-volume surface wave model (FVCOM-SWAVE): Implementation, validations and applications. Ocean Modelling, 28(1), 153–166. https://doi.org/10.1016/j.ocemod.2009.01.007

Qin H., Liu X., Zhang J., Gu W., Su B., He X., Zhang Y., & Zhang X. (2016). Distribution characteristics of petroleum hydrocarbons in seawater of Laizhou bay. Marine Environmental Science, 35(5), 739-742, 755. (In Chinese)

Ralston, D. K., Geyer, W. R., & Lerczak, J. A. (2010). Structure, variability, and salt flux in a strongly forced salt wedge estuary. Journal of Geophysical Research, 115(C6), C06005. https://doi.org/10.1029/2009JC005806

Richards, F. A. (1980). A Compilation of Articles Reporting Research Sponsored by the Office of Naval Research. University of Washington, Department of Oceanography.

Seiler, L., Figueira, R. C. L., Schettini, C. A. F., & Siegle, E. (2020). Three-dimensional hydrodynamic modeling of the Santos-São Vicente-Bertioga estuarine system, Brazil. Regional Studies in Marine Science, 37, 101348. https://doi.org/10.1016/j.rsma.2020.101348

Sharma, V. K., Pant, H. J., Goswami, S., & Bhar, K. K. (2021). Hydrodynamic modeling and radiotracer investigations in Kolkata Port Trust, Kolkata, West Bengal, India. Applied Radiation and Isotopes, 168, 109524. https://doi.org/10.1016/j.apradiso.2020.109524

Shepherd, D., Burgess, D., Jickells, T., Andrews, J., Cave, R., Turner, R. K., Aldridge J., Parker E. R., & Young, E. (2007). Modelling the effects and economics of managed realignment on the cycling and storage of nutrients, carbon and sediments in the Blackwater estuary UK. Estuarine, Coastal

and Shelf Science, 73(3-4), 355-367. https://doi.org/10.1016/j.ecss.2007.01.019

Symonds, A. M., Vijverberg, T., Post, S., Van der Spek, B.-J., Henrotte, J., & Sokolewicz, M. (2017). Comparison between MIKE 21 FM, Delft3D and Delft3D FM FLOW models of Western Port Bay, Australia. Coastal Engineering Proceedings, 35, 11. https://doi.org/10.9753/icce.v35.currents.11

Thompson, B., Hoenicke, R., Davis, J. A., & Gunther, A. (2000). An overview of contaminant-related issues identified by monitoring in San Francisco Bay. Environmental Monitoring and Assessment, 64(1), 409-419. https://doi.org/10.1023/A:1006459605924

Tye, A. M., Rushton, J., & Vane, C. H. (2018). Distribution and speciation of phosphorus in foreshore sediments of the Thames estuary, UK. Marine Pollution Bulletin, 127, 182–197. https://doi.org/10.1016/j.marpolbul.2017.11.044

van de Plassche, O., Chrzastowski, M. J., Orford, J. D., Hinton, A. C., & Long, A. J. (1995). Coastal evolution in the quaternary: IGCP Project 274. Marine Geology, 124(1-4), ix-xii. https://doi.org/10.1016/0025-3227(95)90009-8

Wang, P., Lai, G., & Li, L. (2015). Predicting the Hydrological Impacts of the Poyang Lake Project Using an EFDC Model. Journal of Hydrologic Engineering, 20, 05015009. https://doi.org/10.1061/(ASCE)HE.1943-5584.0001240

Warner, J. C., Geyer, W. R., & Lerczak, J. A. (2005). Numerical modeling of an estuary: A comprehensive skill assessment. Journal of Geophysical Research: Oceans, 110(C5). https://doi.org/10.1029/2004JC002691

Warren, I. R., & Bach, H. K. (1992). MIKE 21: A modelling system for estuaries, coastal waters and seas. Environmental Software, 7(4), 229–240. https://doi.org/10.1016/0266-9838(92)90006-P

Webb, B. W., Phillips, J. M., Walling, D. E., Littlewood, I. G., Watts, C. D., & Leeks, G. J. L. (1997). Load estimation methodologies for British rivers and their relevance to the LOIS RACS(R) programme. Science of The Total Environment, 194–195, 379–389. https://doi.org/10.1016/S0048-9697(96)05377-6

Wei H., Zhao L., Yuan Y., Shi J., Fan X., Liu Z., Wang L., Yuan C., Wang Y., & Wei L. (2010). Study of hydrodynamics and its impact on mariculture carrying capacity of Sanggou Bay：observation and modeling. Progress in Fishery Sciences, (04), 65-71.

Wool, T., Ambrose, R. B., Martin, J. L., & Comer, A. (2020). WASP 8: The Next Generation in the 50-year Evolution of USEPA's Water Quality Model. Water (20734441), 12(5), 1398. https://doi.org/10.3390/w12051398

Wrobel, C. A., & Brebbia, C. A. (Eds.). (2012). Water pollution: Modelling, measuring and prédiction. Springer Science & Business Media.

Wu F. (2020). An investigation of the pollutants discharge control strategies in Xiangshan Bay based on 3D hydrodynamic and water quality numerical modelling. (In Chinese)

Wu G., & Xu Z. (2011). Prediction of algal blooming using EFDC model: Case study in the Daoxiang Lake. Ecological Modelling, 222(6), 1245–1252. https://doi.org/10.1016/j.ecolmodel.2010.12.021

Wu, J. Y., Shen, L., Gao, G., Lin, G. F., Ke, X., & Shen, J. H. (2004). A season-dependent variation of genotoxicity of surface water samples from Taihu Lake, Yangzte delta. Environmental monitoring and assessment, 98(1), 225-234. https://doi.org/10.1023/B:EMAS.0000038188.16088.f3

Xing K., Liu H., & Wu R. (2018). Distribution and Assessment of Petroleum Hydrocarbons in Sea Water of Haikou Bay. Tropical Agricultural Engineering, 42(5), 28-30. (In Chinese)

Xu Z. & Liao Z. (2003). Developing Stages and Spatial Levels of Water Quality Modeling Study. Shanghai Environmental Science, 22(2), 7. (In Chinese)

Xu, M. J., Yu, L., Zhao, Y. W., & Li, M. (2012). The Simulation of Shallow Reservoir Eutrophication Based on MIKE21: A Case Study of Douhe Reservoir in North China. Procedia Environmental Sciences, 13, 1975–1988. https://doi.org/10.1016/j.proenv.2012.01.191

Zhang Q., Tao J., Zhang C., & Qi H. (2018). Analysis on tidal wave propagation characteristics and its influencing factors of Yongjiang River in Zhejiang Province. Ynagtze River, (11), 3-8, 13. (In Chinese)

Zhang, J., Zhang, Z. F., Liu, S. M., Wu, Y., Xiong, H., & Chen, H. T. (1999). Human impacts on the large world rivers: Would the Changjiang (Yangtze River) be an illustration? Global Biogeochemical Cycles, 13(4), 1099–1105. https://doi.org/10.1029/1999GB900044

Zhang, W., Yu, L., Hutchinson, S. M., Xu, S., Chen, Z., & Gao, X. (2001). China's Yangtze Estuary: I. Geomorphic influence on heavy metal accumulation in intertidal sediments. Geomorphology, 41(2), 195–205. https://doi.org/10.1016/S0169-555X(01)00116-7